FINAL TECHNICAL REPORT
DOE/SC0001389

INVESTIGATION OF URANIUM ATTENUATION AND RELEASE AT COLUMN AND PORE SCALES IN RESPONSE TO ADVECTIVE GEOCHEMICAL GRADIENTS

Kaye S. Savage and Wenyi Zhu
Wofford College Environmental Studies Program
429 N. Church Street
Spartanburg, SC 29303

with experimental support from
Mark O. Barnett
Auburn University

Investigation of uranium attenuation and release at column and pore scales in response to advective geochemical gradients

KAYE S. SAVAGE[1*], WENYI ZHU[1], MARK O. BARNETT[2],

[1]Wofford College Environmental Studies, Spartanburg SC, USA, savageks@wofford.edu, rose.zhu@gmail.com
[2]Dept. Civil Engineering, Auburn University, AL, USA, barnem4@auburn.edu

Experimental approach

Column experiments were devised to investigate the role of changing fluid composition on mobility of uranium through a sequence of geologic media. Fluids and media were chosen to be relevant to the ground water plume emanating from the former S-3 ponds at the Oak Ridge Integrated Field Research Challenge (ORIFC) site. Synthetic ground waters were pumped upwards at 0.05 mL/minute for 21 days through layers of quartz sand alternating with layers of uncontaminated soil, quartz sand mixed with illite, quartz sand coated with iron oxides, and another soil layer. Increases in pH or concentration of phosphate, bicarbonate, or acetate were imposed on the influent solutions after each 7 pore volumes while uranium (as uranyl) remained constant at 0.1mM. A control column maintained the original synthetic groundwater composition with 0.1mM U. Pore water solutions were extracted to assess U retention and release in relation to the advective ligand or pH gradients. Following the column experiments, subsamples from each layer were characterized using microbeam X-ray absorption spectroscopy (XANES) in conjunction with X-ray fluorescence mapping and compared to sediment core samples from the ORIFC, at SSRL Beam Line 2-3.

Results

U retention of 55 – 67 mg occurred in phosphate >pH >control >acetate >carbonate columns. The mass of U retained in the first-encountered quartz layer in all columns was highest and increased throughout the experiment. The rate of increase in acetate- and bicarbonate-bearing columns declined after ligand concentrations were raised. U also accumulated in the first soil layer; the pH-varied column retained most, followed by the increasing-bicarbonate column. The mass of U retained in the upper layers was far lower.

Speciation of U, interpreted from microbeam XANES spectra and XRF maps, varied within and among the columns. Evidence of minor reduction to U(IV) was observed in the first-encountered quartz layer in the phosphate, bicarbonate, and pH columns while only U(VI) was observed in the control and acetate columns. In the soil layer, the acetate and bicarbonate columns both indicate minor reduction to U(IV), but U(VI) predominated in all columns. In the ORIFC soils, U was consistently present as U(VI); sorption appears to be the main mechanism of association for U present with Fe and/or Mn, while U occurring with P appears in discrete particles consistent with a U mineral phase. U in soil locations with no other elemental associations shown by XRF are likely uranium oxide phases.

DOE/SC0001389 Final technical report: Investigation of uranium attenuation and release at column and pore scales in response to advective geochemical gradients

K. Savage, W. Zhu, M.O. Barnett

DOE/SC0001389 Final technical report: Investigation of uranium attenuation and release at column and pore scales in response to advective geochemical gradients

1. Introduction

Uranium is a prevalent contaminant in previous uranium mining and milling sites as well as nuclear waste disposal sites such as the Oak Ridge Integrated Field Research Challenge (ORIFRC). In oxidizing environments, uranium usually exists as U(VI) while in reducing environments mostly as less mobile U(IV). Dissolved U(VI) is easily transported in porous media, however, its migration may largely depend on adsorption/precipitation reactions at the surface reactive sites of various minerals, as well as complexation with ligands such as carbonate, phosphate and organic acids from solution. Considering this complicated matrix of solid soil/mineral as well as diverse dissolved ligands, it is critical to construct an appropriate model to predict uranium fate and transport in heterogeneous subsurface media.

Sorption of uranium from aqueous solution on various solid materials has been studied extensively, including iron hydr/oxides, clay, and quartz as well as natural soil and sediments (Lenhart and Honeyman 1999; Arnold, Zorn et al. 2001; Barnett, Jardine et al. 2002; Wazne, Korfiatis et al. 2003; Zheng, Tokunaga et al. 2003; Cheng, Barnett et al. 2004; Payne, Davis et al. 2004; Catalano and Brown 2005; Huber and Lützenkirchen 2009; Korichi and Bensmaili 2009; Kar, Kumar et al. 2011). The adsorption of U(VI) on these solids can be simplified as sorption to hydroxyl groups at reactive surface sites depending on specific characteristics of solid materials (Davis and Kent, 1990). With this simplification, surface complexation models (SCM) can be used to quantitatively describe the uranyl ion sorption on mineral surfaces. Our study applies SCM to the reactive transport of uranium in a stratified column with layered quartz, uncontaminated soil, clay and goethite-coated quartz, which may help to provide insight into uranium attenuation processes in the heterogeneous subsurface environment.

Besides the importance of reactive surfaces on uranium adsorption, ligands from solution may also have huge impacts on uranium migration behavior in the subsurface environment. Carbonate, phosphate and organic acids are common ligands occurring in groundwater and each of them influence uranium adsorption/precipitation processes during transport. For example, in oxidizing environments, U(VI) usually forms uranyl carbonate complexes with carbonate and they are not easily adsorbed to reactive sites on mineral and soil surfaces (Wazne, Korfiatis et al. 2003; Zheng, Tokunaga et al. 2003; Catalano and Brown 2005; Guo, Li et al. 2009). Organic acids can form strong complexes with uranium as well which increases uranium mobility (Lenhart and Honeyman 1999; Murphy, Lenhart et al. 1999; Bednar, Medina et al. 2007; Tokunaga, Wan et al. 2008). On the other hand, phosphate can play a role in inhibiting uranium migration in that it helps to precipitate uranium in solution or facilitate uranium adsorption by forming dominant adsorbed U(VI) surface complex species at low pH on mineral surfaces (Jerden Jr and Sinha 2003; Cheng, Barnett et al. 2004; Jerden Jr and Sinha 2006; Cheng, Barnett et al. 2007; Romero-Gonzalez, Cheng et al. 2007; Guo, Li et al. 2009; Shi, Liu et al. 2009; Singh, Ulrich et al. 2010). The pH of the uranium bearing solutions is also a key parameter that affects uranium migration (Echevarria, Sheppard et al. 2001; Guo, Li et al. 2009).

This study reports on the uranium reactive adsorption/precipitation process in a column system that represents the complicated matrices of real aquifers, with the modification of pH and specific ligands in inlet solutions: carbonate, organic acids (represented by acetate), and phosphate. The utilization of a transport model that incorporates SCM, in combination with observations from synchrotron X-ray microprobe images and X-ray absorption data, help to identify the relative importance of various phenomena to improve predictive models of uranium attenuation and release in natural subsurface environments.

2. Methods

2.1 Column Experiments with advective chemical gradients

Clear polycarbonate columns (4.5 cm ID x 15 cm) were constructed with nine evenly spaced pore water extraction ports using Luer lock fittings sealed with silicone epoxy (Figure 1). Each port consists of a 3.5mm diameter polypropylene tube extending 1.5 cm into each layer, packed with glass wool and capped on the outside. Alternate ports are numbered 1-5 from the bottom to the top of the column; the remaining 4 ports were not used in these experiments and are omitted in the schematic diagram.

All chemicals were certified ACS grade except as noted. Uranium standards and stock solution were prepared from AAS grade uranium standard (1000ppm, J.T. Baker). White quartz sand was obtained from Michaels Stores and sieved to collect a grain size range of approximately 250-500 μm, then rinsed in distilled water. The goethite-coated sand was prepared according to the methods described by Cheng (Cheng, Barnett et al. 2004), who followed Schwertmann and Cornell (1991). Illite-smectite mixed layer clay was obtained from the Clay Minerals Society's Source Clays Repository (ISCz-1, Czechoslovakia) and mixed with the sieved quartz sand in the ratio of 1:4. Soils were collected from a stratigraphically comparable location to the series present at ORNL-ORIFRC, but approximately 8km to the southwest at a location unaffected by the contaminants associated with the ORIFRC (N 35.51261°, W 82.61275°).

Columns were layered with mineral and soil strata; five quartz sand layers (corresponding to locations of ports) sandwiching, from bottom to top, layers of uncontaminated soil, mixed quartz sand and illite, Fe-coated quartz sand, and another layer of uncontaminated soil. Columns were packed by pouring the grains for each layer through a funnel to reach the desired thickness; the mass of each layer is reported in Table 1. Porosity was approximately 32%.

Influent solutions were pumped upward through the columns at 0.05 mL/min using low-flow peristaltic pumps. The columns were pre-conditioned with synthetic groundwater background solution corresponding to a typical groundwater composition from Oak Ridge Area 2 (Table 2) for approximately 72 hours (1 pore volume). Uranium was absent from the background solution. Subsequently, solution concentrations of U were held approximately constant at 0.1 mM. The pH or the concentrations of the ligands of interest (acetate, phosphate, carbonate, added as sodium salts) were increased stepwise after each 7 pore volumes over a 21 day period (Table 3). The pH was adjusted with hydrochloric acid or sodium hydroxide. A non-reactive (KBr) tracer spike was added to the control column influent to determine the dispersion coefficient and verify the uniformity of the packed column.

Pore water was extracted from ports with a 5 mL Luer Lock syringe at designated time intervals (after each 4 pore volumes). Uranium was analyzed by ICP-OES (Varian 710-ES) following 5x – 20x dilution. Acetate and phosphate were analyzed using ion chromatography (Dionex DX-120). The pH was measured using pH test strips due to the small volumes available.

Following the experiments, samples were prepared for microscale characteriztion (see section 2.2) by extruding the material from the columns and using a spatula to transfer approximately 0.15 mg of each reactive layer into a 0.5 mm deep well cut into a polycarbonate plate. The sample was covered with a polypropylene film window (6 μm) attached to the plate with double stick tape and wrapped with a second layer of polypropylene film for containment purposes (SSRL approved sample holder type "4p").

2.2 Microscale characterization of solid samples

X-ray fluorescence microprobe mapping and X-ray absorption spectroscopy were performed at the Stanford Synchrotron Radiation Laboratory, beamlines 10-2 and 2-3. The monochromator was calibrated using Yttrium foil. The monochromator crystal was Si[111] during the data collection on Oak Ridge soils at BL2-3, July 2010, and for all data collected at BL10-2 in July 2011. In July 2011, an Si[220] monochromator was used at BL2-3.

X-ray fluorescence maps were sequentially collected at five energies: 17100 eV, 17170 eV, 17175 eV, 17178 eV, and 17190 eV. These energies correspond respectively to (1) an energy between the Rb K-edge region and the U L(III) edge absorption region; (2) the maximum difference in energy between the U(IV) and U(VI) absorption edges; (3) the U(IV) white line; (4) the U(VI) white line; and (5) a characteristic U(VI) "shoulder" peak related to U-O-U multiple scattering in the uranyl complex. The absorption edge of elemental uranium, for comparison, is 17166 eV. Mapping at these energies permits analysis of the relative proportions of U(IV) and U(VI) in the sample by comparison of intensities at each position on the five different maps, and by principle component analysis for maps of intensity ratios. The maps were collected with raster step sizes of 8-20 μm to achieve map sizes of 0.2 to 2 mm along each edge.

Distribution of Si, P, K, Cr, Mn, Fe, Cu and As+Pb were collected over the map areas by configuring solid-state detector elements to selectively record the fluorescence in their corresponding energy ranges. Data analysis of X-ray fluorescence maps was performed using the computer code SMAK (Sam Webb, SSRL). Elemental correlations and selective elemental map overlays represented as tri-color plots informed interpretation of the XANES spectra.

Map locations for collection of microbeam XANES were chosen on the basis of the relative concentration of uranium as well as correlation of uranium with other elements to obtain a representative set of uranium's geochemical settings within each sample. The spot size was approximately 10 μm. At each location, one to three sweeps were collected over the energy range 17135 eV – 17580 eV ($k=10$ Å^{-1}). Data processing was performed by first using the computer code SIXPACK (Sam Webb, SSRL) to remove channel data with electrical spikes or poor performance, to verify calibration, and to average the sweep data. Then the code ATHENA (Bruce Ravel, Argonne National Laboratories) was used to perform background removal and normalize spectra for plotting.

2.3 Geochemical models

Geochemist's Workbench software (Bethke, 2009) and Visual MINTEQ (Gustafsson, 2010) were used to select the range of solution compositions for advection experiment influent solutions. The target ligand concentrations were each chosen to span a range that predicts both aqueous uranium and uranium mineral phases.

Models combining 1D transport with geochemical reactions, including surface complexation, were generated to simulate the advection experiments by following virtual packets of fluid through the virtual column layers. The code PHREEQC (USGS, Version 2) was applied for modeling calculations and most of the thermodynamic data used were from the WATEQ4f database. Additions to the database were made on the basis of published studies (Guillamont, 2003; Dong and Brooks, 2006; Meinrath and Kimura, 1993;

O'Brien and Williams, 1993; Alwan and Williams, 1980; Gorman-Lewis et al., 2008; Gorman-Lewis et al., 2009; Shvareva et al., 2011; Singh, 2010; , and additional data to describe surface complexation was from Korichi et al (2009), Prikryl et al. (2001), and Cheng et al. (2004). Some of the information used was compiled by Dr. Masa Kanematsu at the University of California, Merced.

3. Results

3.1 Column Experiments with advective chemical gradients

Flow tests were conducted over a 21-day period to investigate the effect of variability in pH and ligand concentrations in synthetic ground water solutions on uranium sequestration through a sequence of previously uncontaminated soil and model mineral layers. Figure 2 shows the breakthrough curve for bromide in the control column. Complete breakthrough was observed after approximately three pore volumes. The dispersion coefficient was estimated to be 3 x 10^{-4} m^2/h using the method of Singh (2002) in which D, the dispersion coefficient, is calculated by the following equation: $D= x^2/4 \pi m^2 t_0^3$, where x is the column length in meters, t_0 is the time corresponding to C/C_0=0.5, and m is the slope of the breakthrough curve at this time. This value provides an average over the entire column; dispersion characteristics of individual layers likely deviate from this value.

3.1.1 Pore water uranium concentration in relation to advective geochemical gradients

Initially, uranium-bearing solutions were pumped upward through all columns and after one pore volume, the ligands of interest were added to each designated influent solution as sodium salts. After times corresponding to 8 and 15 pore volumes, the influent fluids were amended as shown in Table 3. Figure 3 shows the concentration of uranium extracted from each port over time. Port numbers reflect position in the column, from 1 at the bottom to 5 at the top.

Effluent solution compositions were not determined in full due to sample size limitations. Uranium concentration in pore waters varied among the columns over time, indicating the influence of the different ligands and pH. In all columns, pore waters extracted from Port 1 were significantly higher in uranium than in the upper ports, yet much decreased from the influent concentration, indicating sequestration in the lowest quartz layer consistent with visual observation of a yellow precipitate. Solutions extracted from Ports 2 to 5 were generally much lower in uranium (Fig. 3), with the exception of the acetate column.

The acetate column showed a dramatic release (up to 4 times) of uranium after increasing the ligand concentration by 10x at pore volume 15. This held for all five ports. For the carbonate column, after addition of 10x more carbonate into the influent at pore volume 15, the uranium level increased over 5x in the extracted pore water solution at Port 1 but remained stable in the remaining ports. On the contrary, in the phosphate column, no rise in uranium release was observed after the increase of phosphate at pore volume 8 or 15, and the uranium concentration in the extracted solutions decreased slightly. In the pH column, as pH was increased from 4 to 6 at pore volume 8 there was an initial decrease in uranium concentration in ports 1 and 5, followed by stable conditions when pH was increased from 6 to 8 at pore volume 15.

3.1.2 Uranium accumulation in sediments in relation to advective geochemical gradients

The mass of uranium accumulated in each layer over time was calculated according to the differences in uranium concentrations at the extraction ports; hence, the mass reported for Layer 1 refers to the quartz sand beneath Port 1, while Layer 2 includes the quartz sand above Port 1, the first soil layer, and the quartz above the soil but below Port 2; and so on (see Fig. 1). Uranium mass accumulated (or released) in each layer was calculated by multiplying the difference between uranium concentration measured in the higher port and the lower port by flow rate and time passed. The mass of uranium that accumulated in each layer is plotted versus pore volume (corresponding to time) in Figure 4 and tabulated in Table 4. Uranium accumulated mostly in layer 1 (quartz) in all columns. A yellowish precipitate or gel was observed in this layer (all columns) when the columns were dissembled for preparing X-ray fluorescence microprobe mapping samples.

Over all, the phosphate column sequestered the most uranium (38.3 mg) compared to other columns while the carbonate column held the least (29.8 mg). The pH column also accumulated more than 37 mg of uranium while the acetate and control columns each accumulated intermediate quantities (~31 mg). Uranium accumulation increased in all columns over the duration of the experiments (Figure 4) notably influenced by behavior in the lowest quartz layer where most of the uranium was sequestered.

3.2 Microscale characterization

3.2.1 ORIFRC soils

The X-ray fluorescence and XANES data show significant heterogeneity both within individual samples and among samples. Uranium is, in various locations, correlated with Fe, Mn, or both; correlated with phosphorus; or not clearly associated with any of the other mapped elements, where it is interpreted to be present either in association with carbonates, with organic matter, or possibly as a uranium oxide phase. In most cases uranium was identified as U(VI), but evidence of the uranyl complex (shoulder at 17190 eV) was not always indicated. Only in the sample with uranium correlated with phosphorus is there a good indication of a mineral precipitate rather than an adsorbed complex. Figure 5 shows selected X-ray fluorescence maps from sediment cores as tri-color maps to visualize elemental correlations (Fe in red, Mn in blue, U in green; map regions with high correlation of iron and manganese appear magenta). Figure 6 shows the microbeam XANES data, including the spectra associated with areas demarcated on Figure 5.

Sample FWB 236-CT-01 is a grey clay containing rock fragments and hard red aggregates from Area 2. In this clay-rich sample, relatively low uranium is distributed fairly evenly in association with both Mn and Fe. Localized higher uranium areas (Fig. 5A) do not show correlation with any of the other mapped elements. The XANES spectrum (Fig. 6) collected on one of these higher-U areas indicates U(VI), but without the shoulder peak characteristic of the uranyl complex.

The samples described next are all from Area 3. Sample FWB 123-19-00 (Fig. 5B), a medium-dark brown silty clay containing rock fragments that had a recorded activity of 350 cpm, shows high heterogeneity in uranium distribution as well as various degrees of Fe-Mn correlation. For example, at N1 reg 1 little correlation between Fe and Mn is displayed, and the XANES spectrum, collected on the edge of an Fe-rich particle, indicates the presence of the uranyl complex. U occurs with Fe and separate areas at N5 reg 2 and with Mn at N5 reg 3. The XANES from these two areas are similar to one another,

indicating U(VI) but without the uranyl multiple scattering peak. Another area (M1; reg 2&3, not shown) displays an area relatively high in uranium compared with other parts of the sample, here associated primarily with iron; the uranyl complex is indicated in the XANES spectra.

Sample 123-02-00, a hard clay with some rust-red mottling presumed iron oxide, has moderately high uranium concentration throughout. Uranium is most often not associated with any of the other mapped elements in this sample (e.g. M1 reg 2, Figure 5C); however, uranium is associated with Fe in some particles (image not shown; spectrum M3 reg 2 on Fig. 6).

Sample 108-01-00, a dark brown silty clay with greenish rock fragments, displays poorly correlated iron and manganese as shown by distinct red and blue regions where both are shown (Figure 5D). Uranium is associated with Fe (DR reg 1) but not Mn in this sample. At DR reg 2, uranium occurs without Fe or Mn. Both spectra from this sample are similar to those from sample 123-02-00.

Sample 112-10-16, a dark brown silty sand, has ubiquitous uranium but not sufficiently concentrated to obtain XANES data. Uranium is associated with Fe, Mn and Cr (Figure 5E). Lead and/or arsenic are also present in this sample (their fluorescence energies are too similar to distinguish from one another without additional mapping using incident energies below and above their respective absorption edge energies).

Sample 124-18-CT presents the highest uranium concentrations of the samples mapped at SSRL; it has a fine grained dark brown matrix containing rock fragments and calcite precipitates. Unlike in the other samples, here uranium is associated with phosphorus (Figure 5F) and not primarily with iron or manganese. Minor copper and potassium are also present in the high-U region. The high uranium concentration produces relatively smooth XANES spectra, with a strong shoulder peak indicating uranyl. These spectra are interpreted to represent uranyl phosphate precipitates.

3.2.2 Experimental column sediments

An array of microbeam XRF maps is shown in Figure 7, and XANES spectra are presented in Figure 8. The XRF microprobe maps and XANES spectra indicate differences in uranium distribution and speciation amongst and within the columns. Interpretation of these differences are explored in the discussion. Some features, however, were common to all columns.

In all of the columns, pore water data (Fig. 3), direct observation of a yellow substance in quartz layer 1, and XRF maps (Fig. 7) indicate significant sequestration of uranium in the layer first encountered by the influent. Microbeam XANES spectra collected at accumulations on quartz grains in these base layers show similar spectral features among the columns and indicate U(VI). The spectral features do not indicate long-range order, and given the time frame of the experiments, these precipitates are interpreted to be amorphous uranium oxides in all columns.

The Fe-coated quartz layer does not show significant adsorption of uranium in any of our experimental columns, even though it was reported that Fe oxides can considerably modify uranium sorption behavior even when they are not present in major phases (*Payne et al, 1998*… and) (Qafoku and Icenhower 2008).

However, iron was detected at lower levels than expected in X-ray fluorescence microprobe mapping of the Fe coated quartz sand; this may attribute to absence of uranium adsorption onto this mineral layer.

4 Discussion and geochemical models

Abundant investigations regarding uranium adsorption/desorption to various mineral surfaces such as goethite, clay, quartz and soil as well as soil and sediments have been carried out. However, the utilization of a stratified column with different mineral materials (quartz, clay, goethite, soil) in an advective uranium transport experiment hasn't been addressed. In natural environments, where the geochemical settings are complicated and heterogeneous, it is reasonable to expect a multilayered aquifer when considering the fate and transport of contaminants in the subsurface. By combining information from geochemical models with observations from synchrotron X-ray microprobe and X-ray absorption spectroscopy, we may gain a better understanding of the influence of ground water composition on the behavior of uranium in heterogeneous settings.

The measured pore water uranium concentrations, cation and ligand concentrations from influent solutions, and pH were explored in relation to geochemical speciation models incorporating surface complexation as well as precipitation and dissolution to predict and interpret uranium sequestration and release. Results of a 1D transport model, using the computer code PHREEQC to simulate advective uranium transport in the columns, are discussed below. Partial output files that summarize the input used to produce the models shown in Figure 9 are included in Appendix A.

4.1 Variability in column experiments

The possible causes of variability in U speciation and distribution among the five experimental columns are (1) differences in ligand behavior; (2) differences in stability of various forms of adsorbed and/or precipitated uranium under particular column conditions; (3) differences in flow patterns. The rate of flow in all five columns remained nominally constant over the length of the experiments and, while preferential flow path development is possible, no evidence of preferential flow paths was observed. Hence the models focus on geochemical rather than hydraulic heterogeneity.

4.1.1 Control column and features common to all columns

The control column was used to optimize baseline reactive transport model conditions before attempting to model columns with advective chemical gradients. Equilibrium phases (mineral content) were defined for each layer. The base quartz layer was treated as two sub-layers due to the observation of precipitates in the lower part of each column, so that ten layers total were included in the models. Model surfaces with sorption sites were also defined for each layer. The virtual surface library included silica (Prikryl et al., 2001), alumina (Korichi et al., 2009), hydrous ferric oxide (hereafter denoted HFO) (Cheng et al., 2004), and generic "soil." Both HFO and soil surfaces incorporated "strong" and "weak" adsorption sites. All of the virtual surfaces allowed for sorption of the uranyl ion including complexation with hydroxyls. The virtual HFO and soil surfaces also allowed for uranyl ternary complexes with carbonate.

The advecting fluid was treated as packets advancing through the column, reacting within each defined layer and then moving into the succeeding layer with a new composition. The virtual column was initially

"filled" with groundwater of background composition without added uranium prior to introducing the virtual U-bearing solution. 210 time steps of 8640 seconds each accounted for the 21 days for each experiment (i.e., ten fluid packet shifts per day, each 2.4 hours long). Virtual influent compositions were changed in accordance with experimental conditions at pore volumes 8 and 15 in the pH, acetate, phosphate, and bicarbonate column models.

Because there are many uranium phases, and XANES data did not indicate sufficient long-range order to identify specific phases actually present, the phases permitted to precipitate under calculated equilibrium conditions in the models were selected from among the phases reported as supersaturated in initial modeling efforts. Supersaturation is not a sufficient condition for precipitation because of kinetic inhibitions. Selection criteria favored commonly reported phases; these were then allowed or dismissed in the initial modeling efforts until results were similar to the experimental observations (Figure 9A) for both uranium concentrations and pH in the control column. Precipitation of particular phases incorporated in the models is not meant to suggest that these are the actual phases that precipitated under experimental conditions.

In the control column and in the other columns prior to the experimental additions, when the initial model influent encounters virtual quartz layer 1, positive saturation indices for uranium minerals from high to low are becquerelite ($Ca(UO_2)_6O_4(OH)_6 \cdot 8(H_2O)$), compreignacite ($K_2(UO_2)_6O_4(OH)_6 \bullet 8(H_2O)$), uranophane ($CaH_2(SiO_4)_2(UO_2) \bullet 5(H_2O)$), $CaUO_4$, soddyite ($(UO_2)_2SiO_4 \cdot 2H_2O$), and schoepite ($(UO_2)_8O_2(OH)_{12} \cdot 12H_2O$). Of these, permitting precipitation for any except schoepite causes the simulated dissolved uranium level to drop far below that observed in our solutions, suggesting that these minerals are not forming in the columns. Schoepite was permitted to virtually precipitate to achieve a saturation index of +0.1 (i.e., forcing the simulated solution to remain slightly supersaturated). Following the initial virtual precipitation of schoepite, this mineral does not become supersaturated again in the simulated pore fluids anywhere in the simulated control column. The uranium associated with the schoepite precipitate in the model reaches approximately 22 mg in the first quartz layer, which is reasonably consistent with the actual calculated mass in this layer (31 mg). An additional 6.6 mg is modeled to precipitate in the first soil layer, and 2 mg in the illite layer; these are higher than the calculated masses of 2.2 and 0.2 mg, respectively. The minor remaining uranium sequestration in the modeled column is associated with silica surface sites (throughout), alumina surface sites (soil and clay layers), and HFO (soil and goethite layers). All of the modeled surface sites combined account for approximately 0.4 mg of uranium sequestration, of which nearly half is on surface sites within the lower soil layer.

The low flow rate used in this experiment (0.05mL/min) may also contribute to the low recovery of uranium in the extracted pore water solutions. It is reported that there is a strong tendency of uranium adsorb to inner surface of reaction vessels under conditions of very low pore water velocity (Romero-Gonzalez, Cheng et al. 2007). However, the low pore water velocity was selected to better mimic groundwater flow. Some portion of the yellow precipitates observed were on the bottom of the columns in association with silicon gel used as a sealant, which may also have contributed to to low uranium recovery. In our experiments, the Fe coated quartz layer generally does not show significant adsorption of uranium, although it has been reported that Fe oxides can considerably modify uranium sorption behavior even when they are not present in major phases (Qafoku and Icenhower 2008). This is possibly due to the already very low uranium concentration after passing through previous layers (except see the acetate column description, section 4.1.2).

4.1.2 Acetate-bearing column

The acetate-bearing column behavior was similar to that of the control column in the first part of the experiment and after increasing the ligand concentration from 10^{-5} to 10^{-4} M at pore volume 8. However, after increasing the ligand concentration by another 10x at pore volume 15, the uranium concentration dramatically increased in all five ports (Fig 3a), becoming the highest in any of the five columns. The uranium that was transferred upwards in pore waters permitted more to accumulate in the uppermost layers compared with the other columns.

The reactive transport model was generated using the same parameters as the control column model, but with increases in acetate at the appropriate time steps (PV8 and PV 15). The model captures the rising trend in pore water uranium after PV 15, but underestimates the concentrations. pH values are reasonable and trend correctly for the base layer quartz sand. However, pH trends after the second increase in acetate concentration at PV 15 are not captured for layers 2 and 3 (soil, illite).

Acetate as a ligand to mobilize uranium has not been widely discussed. However, research has shown that other types of organic matter such as humic acids can impact uranium sorption in aquifer environments, and that it is mostly dependent upon pH. Under acidic conditions, organic acids can strongly adsorb onto mineral phases and complex ions such as UO_2^{2+}(Wan, Dong et al. 2011). However, our observations showed higher acetate may help to increase uranium mobility even under acidic conditions, in contrast to humic acid.

X-ray absorption spectra from the acetate column showed only U(VI). Oscillation in the low-K EXAFS region suggest that longer-range order is present in the precipitate in the lowest quartz layer than was the case in the control column. It is possible that acetate may promote crystallization, but more work would be needed to clarify this behavior. It is also possible for acetate to be used as a electron donor for U(VI) reduction and thus to promote uranium sequestration; however, we did not observe this behavior. This may be due to the lack of active microorganisms that could catalyze uranium reduction in our layered soil/mineral column.

4.1.3 Bicarbonate-bearing column

For the bicarbonate column, uranium release remained fairly stable upon increasing the inlet ligands to 10^{-3}M at pore volume 8. After addition of 10x more bicarbonate (10^{-2} M) into the influent, the uranium level increased over 5x from the extraction solution at port 1 (Fig 3). As in the acetate case, the reactive transport model captures some of the uranium concentration trends (Fig. 9); however, in this case the model overestimates rather than underestimates the increased concentration at high bicarbonate levels. The trends in pH are comparable to those for the acetate column for the first 15 pore volumes. Following the second increase in bicarbonate, the pH model does not capture the trend in the quartz base layer, but more closely approximates the soil and illite layers than did the acetate model. The XANES spectrum collected from the carbonate column's quartz layer 1 indicates both U(IV) and U(VI), and the X-ray

fluorescence map shows localized high uranium concentrations consistent with the presence of a precipitate.

The decrease in pore water uranium in Port 1 following the first increase in bicarbonate concentration may be due to the formation of additional precipitates (modeled as schoepite, see section 4.1.1) as well as complexation of uranyl ions on quartz surfaces. The rate of accumulation of uranium in the base quartz layer declines slightly compared with the other columns; however, the uranium that does move upward following the second increase in bicarbonate concentration becomes sequestered in the soil layer (and to a very limited extent in the illite/quartz layer; Fig. 4), such that there is almost no uranium mobility through the upper layers.

It has been shown that carbonate ions can form complexes with uranium that promote its mobility by inhibiting adsorption (Germanicova and Lubal 2006; Suzuki, Abdelouas et al. 2006; Um, Serne et al. 2007). Moreover, if calcium is available, the desorption of uranium-carbonate ternary complexes from soil and minerals may be enhanced (Zheng, Tokunaga et al. 2003). Our observations are consistent with this increased mobility; however, upon transfer into a layer with ample surface sites available (e.g. our soil layer), the uranium was captured. Our data does not permit interpretation of the specific complexes involved in this sequestration.

4.1.4 Phosphate-bearing column

There are two processes of uranium retained in unsaturated soil: by incorporation into phosphate minerals and/or adsorbed with phosphorous onto iron oxides that coat the surface on other soil minerals (Jerden Jr and Sinha 2006). In our column study, since there were no iron oxides presented in the first few layers, it was more likely that the uranium attenuation was due to the precipitation of uranium with phosphate. By the time that the fluid reached the goethite-coated quartz layer, there was not sufficient uranium remaining in solution to accumulate (Fig. 4).

In the phosphate column's base quartz layer, uranium mobility initially rose, then decreased after raising the phosphate level from 0.005 to 0.01 mM at pore volume 8. With the addition of additional phosphate (to reach 0.05 mM), uranium concentrations stabilized. The geochemical model (Fig. 9) does not well capture these features, and suggests increased mobility that was not observed after the second phosphate increase. Of the minerals in the databased used for these models, only hydrated autunite was shown to be supersaturated, but permitting its precipitation did not improve the model fits. This suggests that another phase not included in the model might control the uranium concentrations in the presence of higher phosphate (Jerden Jr and Sinha 2006; Wellman, Gunderson et al. 2007). Indeed, the XANES spectra indicate that some of the uranium in the base quartz layer is present as U(IV), with some evidence of ordered behavior, and the XRF map shows a correlation between U and P. The lack of a reductant in the model may be the reason that an appropriate phase did not appear to be supersaturated. Additional modeling work to better decipher what may have contributed to the reducing conditions would be helpful, particularly since others have found that once uranium phosphate precipitates are formed, they do not easily change in response to oxidizing conditions and may become a sink for uranium in the long term (Beazley, Martinez et al. 2011). It is also reported that phosphate inhibits uranium release from sediments in which uranium can be adsorbed to the secondary phosphate precipitates (Shi, Liu et al. 2009).

4.1.5 pH column

In the pH column, pH was increased from 4 to 6 and from 6 to 8, at pore volumes 8 and 15, respectively. The initial fluid in the column was the same as in the other columns prior to introducing the pH 4 fluid; this seems to have influenced the early pH via mixing so that the lowest pH recorded during this initial time was actually 6.1, two full units above the intended value. The uranium concentrations in pore waters extracted at Ports 1 and 5 increased at first and then decreased, then remained stable for the duration of the experiment when pH was raised to 6 and then to 8. The geochemical model captured the initial uranium increase in the base quartz layer well (Fig. 9), but overpredicted the early concentrations in the soil and illite layers. However, the model is reasonably close to measured concentrations after PV 8 in all three of these layers. The pH recorded in the model is a poor match to the data. Although the initial pH values modeled for the base quartz layer and the illite layer were on target, there was immediate divergence from the measured values. After PV 8, the base layer quartz model matches well to the data, but the pH variability in the other two layers is not matched in the model.

Higher pH is reported to immobilize uranium (Beazley, Martinez et al. 2011). With higher pH, uranium is more likely to form uranyl oxides and adsorb to minerals which leads to uranium attenuation. The base quartz layer of our column is consistent with this phenomenon. Inconsistencies might be due to local micro-environments where pH may not have been as uniform as intended. The pH column demonstrated one XANES spectrum with U(VI) only and a high localized concentration suggesting a short-range ordered precipitate, and one spectrum with U(IV) and U(VI) with much lower concentration (based on signal: noise ratio), suggesting adsorbed species.

4.2 Implications for subsurface environments and the ORIFRC

Two processes predominantly control the attenuation of uranium. One is to form uranium complexes onto surface sorption sites on minerals or soils; uranium can also precipitate in the presence of ligands or become incorporated into other precipitated minerals. We found that at high uranium concentrations, quartz sand generally provided an effective environment for attenuation except in the presence of high concentrations of acetate or bicarbonate. Our findings also indicate that the attenuation and release of uranium in a column with layered strata may largely depend on the composition of influent solutions as well as pH. Uranium mobility was promoted by high concentrations of acetate and bicarbonate, and inhibited at higher pH values. The role of phosphate was more clearly dependent on oxidation conditions that were not reproduced in our models.

Higher levels of phosphate may help to retain uranium by formation of precipitates, while higher levels of carbonate and acetate facilitate the transportation of uranium by forming strong complexes that decrease adsorption onto mineral surfaces. In summary, the advective chemical gradient column experiment and the associated models may help improve prediction of the attenuation of dissolved uranium in response to gradients in pH, carbonate, phosphate and organic carbon, in uranium-contaminated heterogeneous media sites such as the Oak Ridge Integrated Field Research Challenge (ORIFRC).

5 References

Alwan, A.A. and P.A. Williams (1980). “The aqueous chemistry of uranium minerals 2: Minerals of the liebigite group.” Mineralogical Magazine 47: 65-67

Arnold, T., T. Zorn, et al. (2001). "Sorption behavior of U(VI) on phyllite: experiments and modeling." Journal of Contaminant Hydrology 47(2鈥?): 219-231.

Barnett, M. O., P. M. Jardine, et al. (2002). "U(VI) adsorption to heterogeneous subsurface media: Application of a surface complexation model." Environmental Science & Technology 36(5): 937-942.

Beazley, M. J., R. J. Martinez, et al. (2011). "The effect of pH and natural microbial phosphatase activity on the speciation of uranium in subsurface soils." Geochimica et Cosmochimica Acta 75(19): 5648-5663.

Bednar, A. J., V. F. Medina, et al. (2007). "Effects of organic matter on the distribution of uranium in soil and plant matrices." Chemosphere 70(2): 237-247.

Bethke, C.M. and S. Yeakel, 2009, “The Geochemist’s Workbench, Version 8.0,” Hydrogeology Program, University of Illinois, Urbana.

Catalano, J. G. and G. E. Brown (2005). "Uranyl adsorption onto montmorillonite: Evaluation of binding sites and carbonate complexation." Geochimica Et Cosmochimica Acta 69(12): 2995-3005.

Cheng, T., M. O. Barnett, et al. (2004). "Effects of Phosphate on Uranium(VI) Adsorption to Goethite-Coated Sand." Environmental Science & Technology 38(22): 6059-6065.

Cheng, T., M. O. Barnett, et al. (2007). "Reactive transport of uranium(VI) and phosphate in a goethite-coated sand column: An experimental study." Chemosphere 68(7): 1218-1223.

Echevarria, G., M. I. Sheppard, et al. (2001). "Effect of pH on the sorption of uranium in soils." Journal of Environmental Radioactivity 53(2): 257-264.

Germanicova, M. and P. Lubal (2006). "Spectrophotometric determination of uranium(VI) in the presence of carbonates and oxalates and its application to uranium(VI) speciation analysis." Chemicke Listy 100(9): 821-827.

Gorman-Lewis, D., J.B. Fein, P.C. Burns, J.E.S. Szymanowksi and J. Converse (2008). “Solubility measurements of the uranyl oxide hydrate phases metaschoepite, compreignacite, Na-compreignacite, becquerelite, and clarkeite.” J. Chemical Thermodynamics 40:980-990.

Gorman-Lewis, D., P.C. Burns, and J.B. Fein (2008). “Review of uranyl mineral solubility measurements.” J. Chemical Thermodynamics 40:335-352.

Gorman-Lewis, D., et al. (2009). “Thermodynamic Properties of Autunite, Uranyl Hydrogen Phosphate, and Uranyl Orthophosphate from Solubility and Calorimetric Measurements,” Environmental Science & Technology. 43(19):7416-7422.

Guillamont, R., Fanghanel, Th., Fuger, J. et al. (2003). “Update on the chemical thermodynamics of uranium, neptunium, plutonium, americium, and technetium.” Nuclear Energy Agency Data Bank, Organization for Economic Cooperation Development, vol. 5 of Chemical Thermodynamics, Amsterdam, Elsevier.

Guo, Z., Y. Li, et al. (2009). "Sorption of U(VI) on goethite: Effects of pH, ionic strength, phosphate, carbonate and fulvic acid." Applied Radiation and Isotopes 67(6): 996-1000.

Gustafsson, J. P. "Visual MINTEQ ver. 3.0.," 2010.

Huber, F. and J. Lützenkirchen (2009). "Uranyl Retention on Quartz—New Experimental Data and Blind Prediction Using an Existing Surface Complexation Model." Aquatic Geochemistry 15(3): 443-456.

Jerden Jr, J. L. and A. K. Sinha (2003). "Phosphate based immobilization of uranium in an oxidizing bedrock aquifer." Applied Geochemistry 18(6): 823-843.

Jerden Jr, J. L. and A. K. Sinha (2006). "Geochemical coupling of uranium and phosphorous in soils overlying an unmined uranium deposit: Coles Hill, Virginia." Journal of Geochemical Exploration 91: 56-70.

Kar, A. S., S. Kumar, et al. (2011). "U(VI) sorption by silica: Effect of complexing anions." Colloids and Surfaces A: Physicochemical and Engineering Aspects 395(0): 240-247.

Korichi, S. and A. Bensmaili (2009). "Sorption of uranium (VI) on homoionic sodium smectite experimental study and surface complexation modeling." Journal of Hazardous Materials 169: 780-793.

Lenhart, J. J. and B. D. Honeyman (1999). "Uranium(VI) sorption to hematite in the presence of humic acid." Geochimica et Cosmochimica Acta 63: 2891-2901.

Meinrath, G., and T. Kimura (1993). "Carbonate complexation of the uranyl(VI) ion." Journal of Alloys and Compounds 202:89-93.

Murphy, R. J., J. J. Lenhart, et al. (1999). "The sorption of thorium (IV) and uranium (VI) to hematite in the presence of natural organic matter." Colloids and Surfaces A: Physicochemical and Engineering Aspects 157(1鈥?): 47-62.

O'Brien, T.J. and P.A. Williams (1993). "The aqueous chemistry of uranium minerals 4: Schrockingerite, grimselite, and related alkali uranyl carbonates." Mineralogical Magazine 47: 69-73

Payne, T. E., J. A. Davis, et al. (2004). "Surface complexation model of uranyl sorption on Georgia kaolinite." Applied Clay Science 26(1鈥?): 151-162.

Prikryl, J.D., A. Jain, R.T. Pabalan, and D.R. Turner (2001). "Uranium (VI) sorption behavior on mixed silicate minerals." Journal of Contaminant Hydrology 47: 241–253.

Qafoku, N. and J. Icenhower (2008). "Interactions of aqueous U(VI) with soil minerals in slightly alkaline natural systems." Reviews in Environmental Science and Biotechnology 7(4): 355-380.

Romero-Gonzalez, M. R., T. Cheng, et al. (2007). "Surface complexation modeling of the effects of phosphate on uranium(VI) adsorption." Radiochimica Acta 95(5): 251-259.

Schwertmann, U.; Cornell, R.M. Iron oxides in the laboratory, VCH: New York, 1991.

Shi, Z. Q., C. X. Liu, et al. (2009). "Inhibition Effect of Secondary Phosphate Mineral Precipitation on Uranium Release from Contaminated Sediments." Environmental Science & Technology 43(21): 8344-8349.

Shvareva, T.Y., L. Mazeina, D. Gorman-Lewis, P. Burns, J.E.S. Szymanowski, J.B. Fein and A. Navrotsky (2011). "Thermodynamic characterization of boltwoodite and uranophane: Enthalpy of formation and aqueous solubility." Geochimica Et Cosmochimica Acta 75:5269-5282.

Singh, A., K. U. Ulrich, et al. (2010). "Impact of phosphate on U(VI) immobilization in the presence of goethite." Geochimica Et Cosmochimica Acta 74(22): 6324-6343.

Singh, S. K. (2002). "Estimating Dispersion Coefficient and Porosity from Soil-Column Tests." J. Environ. Eng. 128: 1095.

Suzuki, T., A. Abdelouas, et al. (2006). "Oxidation and dissolution rates of UO2(s) in carbonate-rich solutions under external alpha irradiation and initially reducing conditions." Radiochimica Acta 94(9-11): 567-573.

Tokunaga, T. K., J. M. Wan, et al. (2008). "Influences of Organic Carbon Supply Rate on Uranium Bioreduction in Initially Oxidizing, Contaminated Sediment." Environmental Science & Technology 42(23): 8901-8907.

Um, W., R. J. Serne, et al. (2007). "U(VI) adsorption on aquifer sediments at the Hanford Site." Journal of Contaminant Hydrology 93(1-4): 255-269.

United States Geological Survey, http://wwwbrr.cr.usgs.gov/projects/GWC_coupled/phreeqc/

Wan, J. M., W. M. Dong, et al. (2011). "Method to Attenuate U(VI) Mobility in Acidic Waste Plumes Using Humic Acids." Environmental Science & Technology 45(6): 2331-2337.

Wazne, M., G. P. Korfiatis, et al. (2003). "Carbonate Effects on Hexavalent Uranium Adsorption by Iron Oxyhydroxide." Environmental Science & Technology 37(16): 3619-3624.

Wellman, D. M., K. M. Gunderson, et al. (2007). "Dissolution kinetics of synthetic and natural meta-autunite minerals, X-3-n((n)+) [(UO_2)(PO_4)](2)•H_2O, under acidic conditions." Geochemistry Geophysics Geosystems 8.

Zheng, Z., T. K. Tokunaga, et al. (2003). "Influence of Calcium Carbonate on U(VI) Sorption to Soils." Environmental Science & Technology 37(24): 5603-5608.

Table 1. Masses (g) of sediment layers in advective gradient column experiments

Target ligand:	control	pH	acetate	carbonate	phosphate
Quartz (top)	50.9	58.0	50.3	62.5	58.6
Soil	25.2	25.1	25.1	24.9	24.7
Quartz	39.6	37.9	40.9	40.6	40.2
Goethite + Quartz	28.4	30.7	36.0	35.0	40.0
Quartz	45.6	44.6	40.0	45.4	36.1
Clay + Quartz	30.7	30.7	31.2	31.8	30.2
Quartz	45.4	45.1	44.9	45.1	38.8
Soil	25.1	25.1	25.1	26.5	25.0
Quartz (bottom)	50.0	50.1	50.0	50.1	50.1

Table 2. Components of synthetic ground water used in advective chemical gradient experiments. Solution pH is 5.2.

Reagent	Concentration (mM)
$MgSO_4$	0.66
$Ca(NO_3)_2$	3.34
KCl	0.14
$MgCl_2$	0.44
NaCl	1.29

Table 3. Amendments to synthetic ground water solutions in four columns after 2, 9, and 16 pore volumes. A control column remained unamended throughout the duration of the experiments.

Target ligand:	pH	acetate (mMol)	bicarbonate (mMol)	phosphate (mMol)
PV 0	4.06	0	0	0
PV 2	5.62	0.01	0.10	0.005
PV 8	8.16	0.1	1	0.01
PV 15	9.69	1	10	0.05
Adjusted using:	NaOH	$NaCH_3COO$	Na_2CO_3	$NaH_2PO_4 \bullet H_2O$

Table 4. Uranium mass accumulation in columns in relation to pore volumes of fluid (mg)

Pore Volume	Control	Phosphate	Carbonate	Acetate	p H
1	1.5	1.8	1.4	1.5	1.8
4	5.9	7.3	5.7	5.9	7.0
8	11.8	14.6	11.3	11.8	14.0
11	16.3	20.0	15.6	16.2	19.4
15	22.2	27.3	21.3	22.1	26.4
18	26.7	32.8	25.5	26.4	31.7
21	31.1	38.3	29.8	30.8	37.1

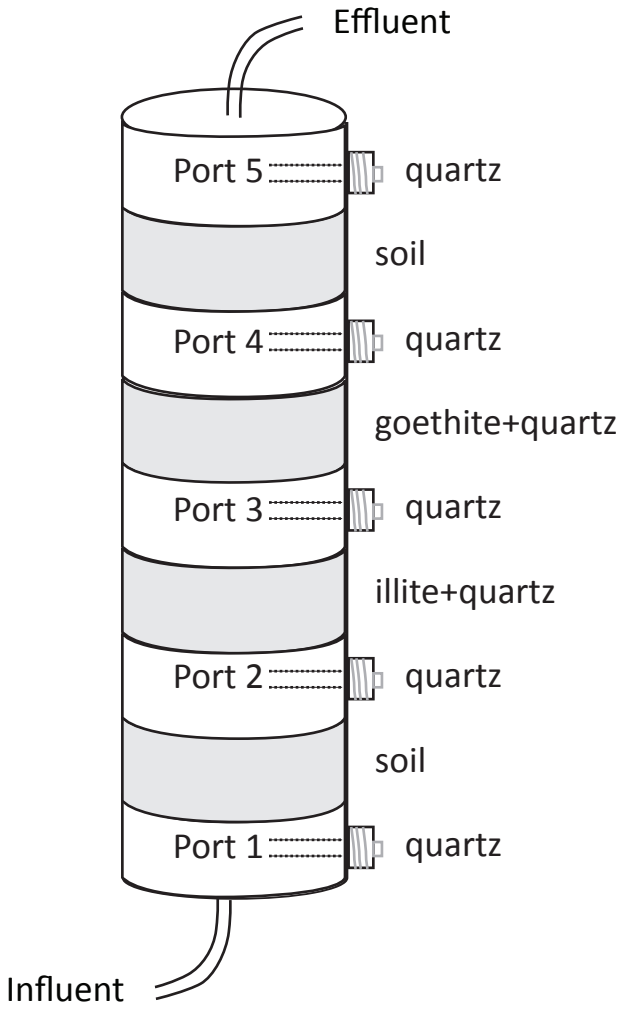

Figure 1. Schematic of column used in advective gradient experiments.

Figure 2. Bromide breakthrough curve used to estimate the dispersion coefficient.

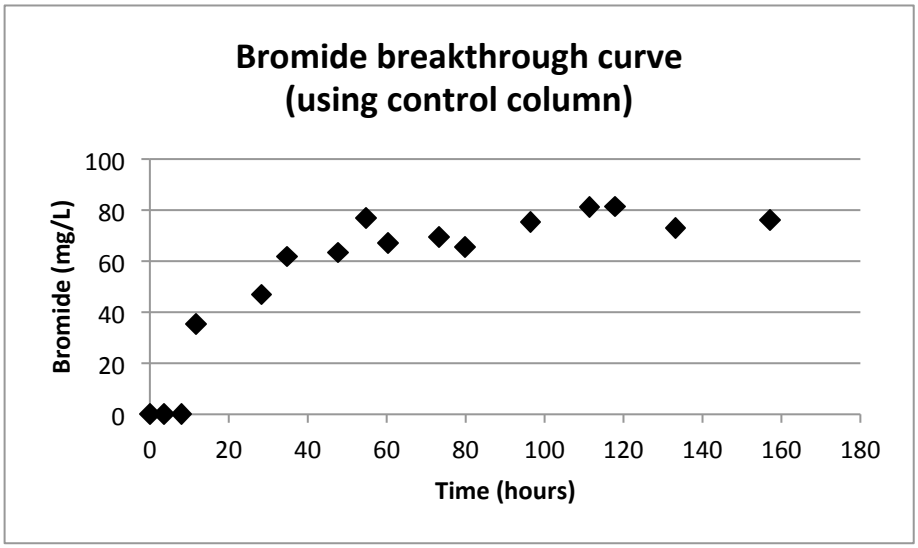

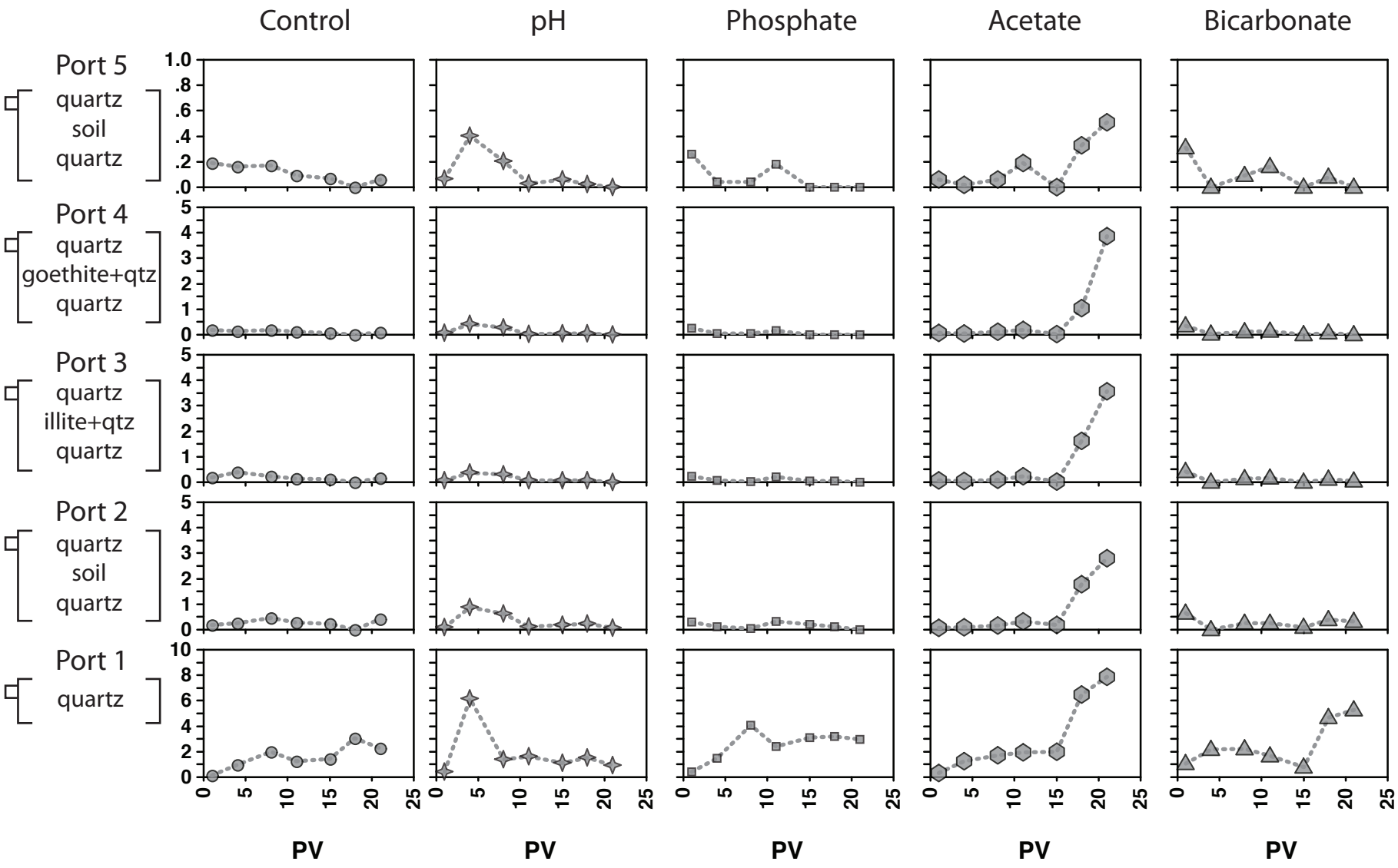

Figure 3. Concentration of uranium (mg/L) in pore waters in column experiments in relation to pore volumes of fluid passed.

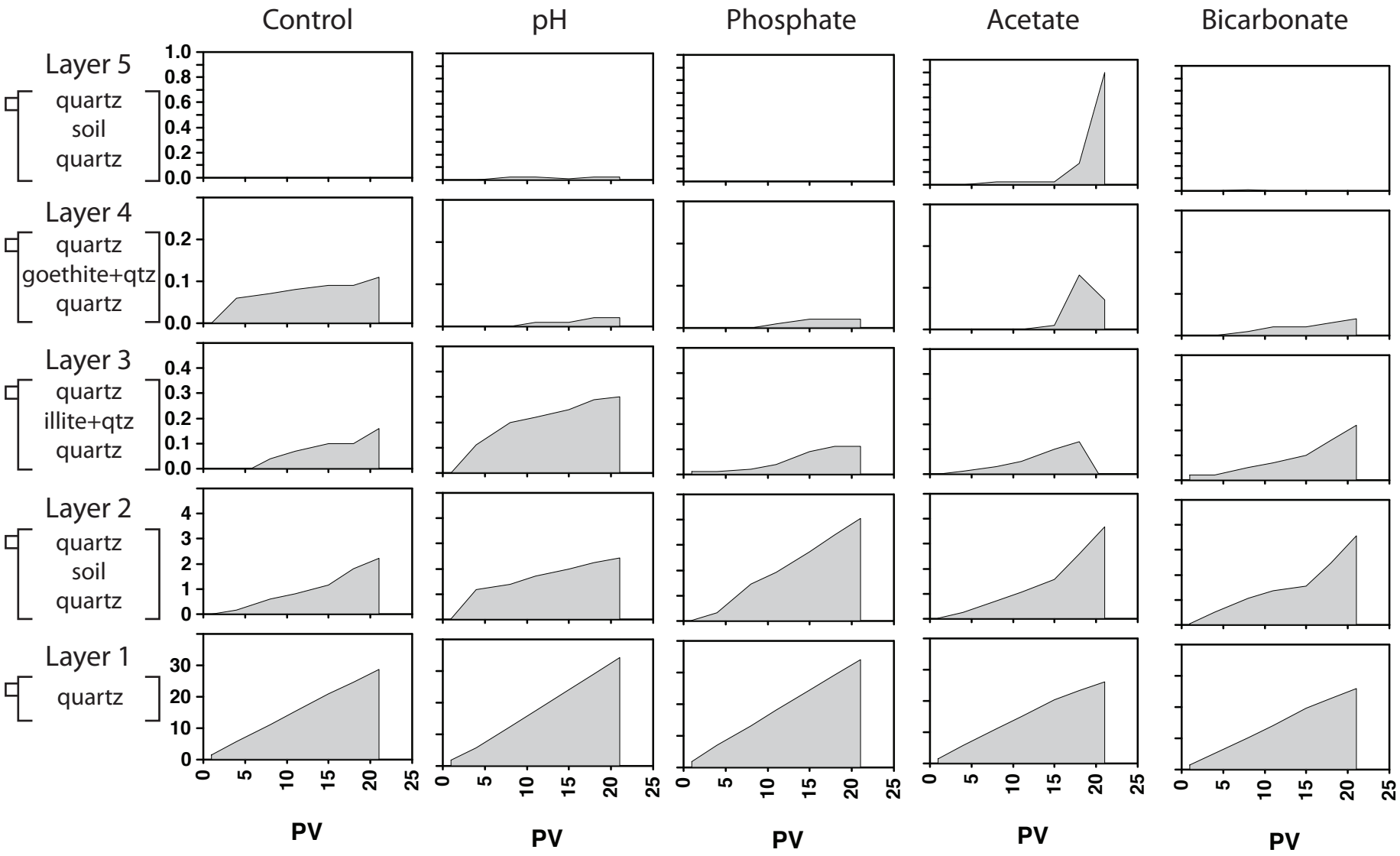

Figure 4. Calculated mass of uranium (mg) accumulated in layered column experiments in relation to pore volumes of fluid passed.

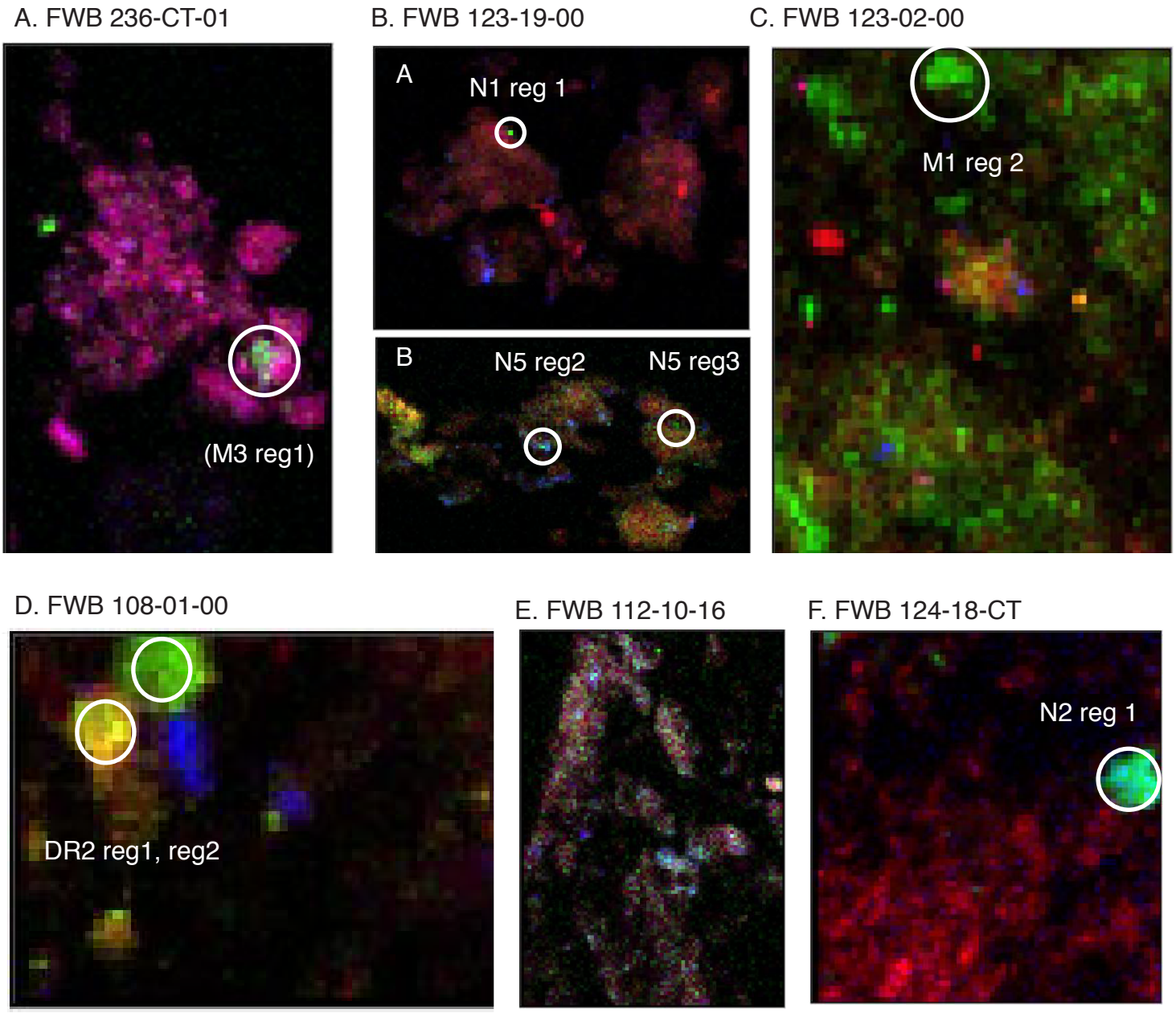

Figure 5. Tricolor maps showing elemental distributions on selected areas of samples collected at Oak Ridge FRC. Iron is represented in red, manganese in blue, and uranium in green; combined colors indicate the presence of one or more of these. White circles show locations of XANES spectra shown in Figure X. In (F) FWB 124-18-CT, blue represents phosphorus rather than manganese.

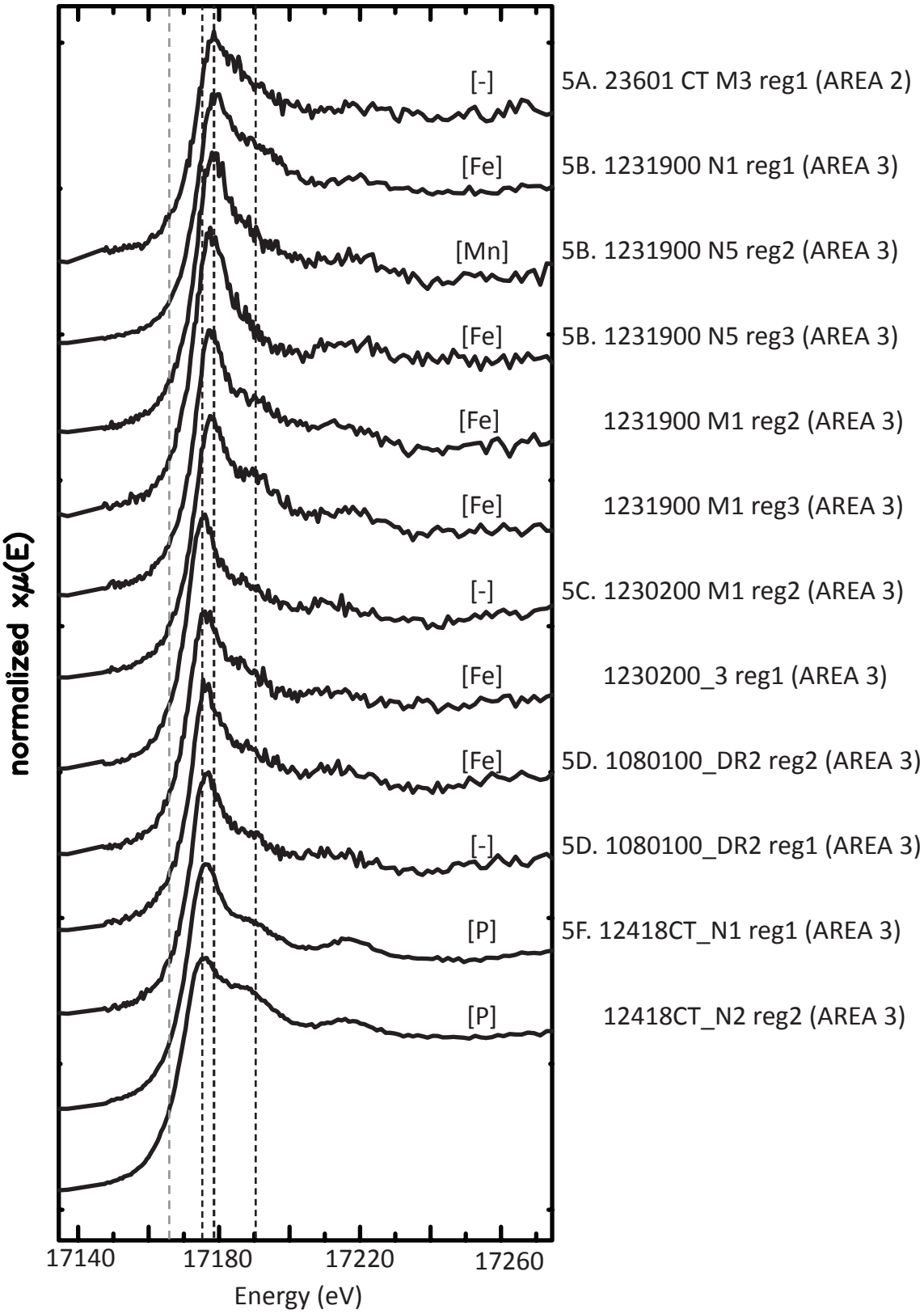

Figure 6. X-ray absorption near-edge spectra (XANES) collected on archived sediment samples from ORNL. The bracket shows the predominant correlating element at each location. To the right the sample name and XRF map area is indicated; those shown in Figure 5(A-F) are noted. Area 2 and Area 3 refer to the neutral pH gravel pathway and the low pH shale pathway away from the former S-3 ponds, respectively. Vertical dashed lines indicate, from low to high energy, 17166 eV U(0) edge position; 17175 eV position of U(IV) white line; 17178 eV position of U(VI) white line; 17190 eV position of "shoulder" indicating uranyl.

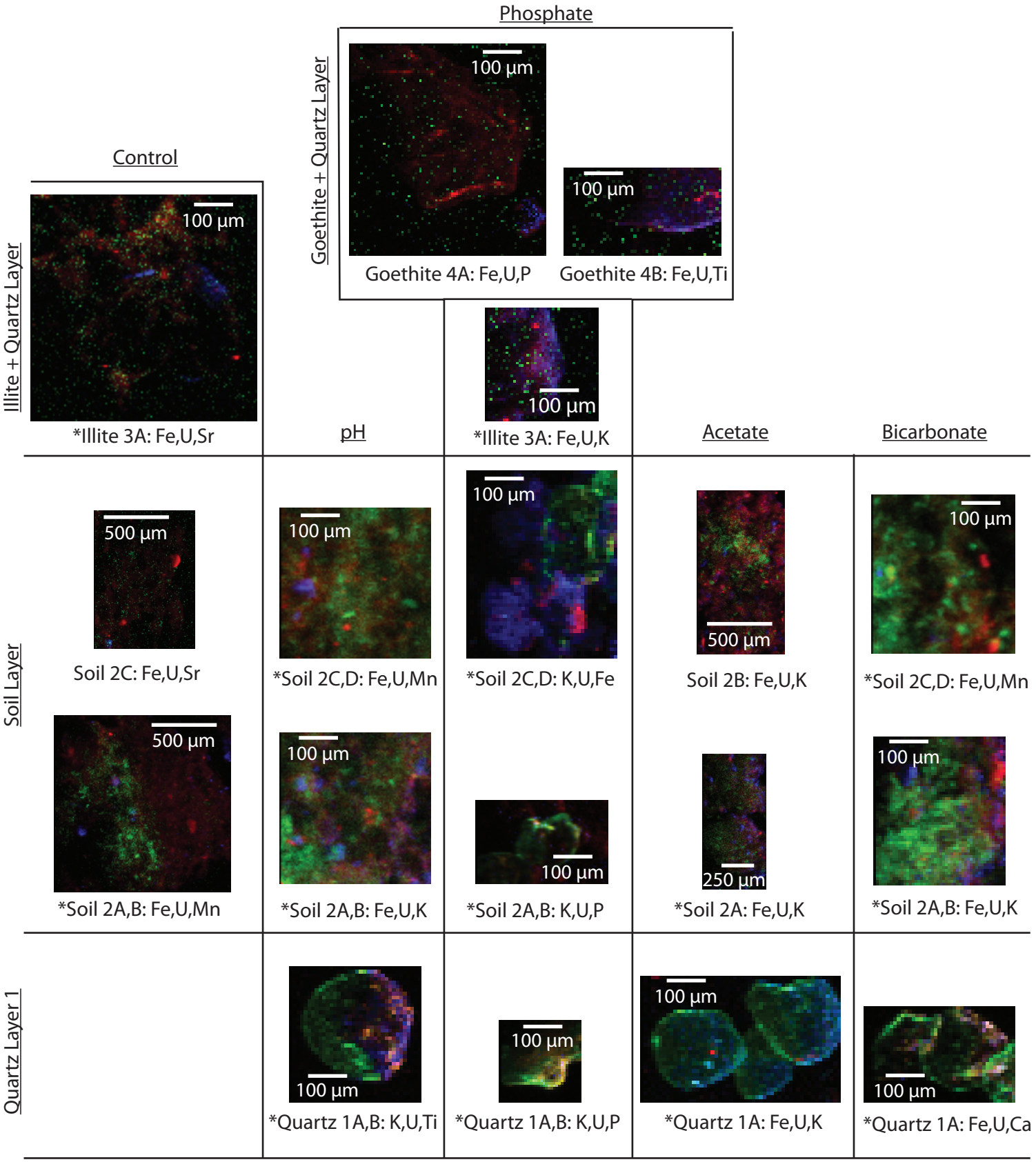

Figure 7. Microbeam XRF maps of experimental samples. Starred samples have associated XANES spectra shown in Figure 8. In each description, the first element is shown in red, the second (uranium) in green, and the third in blue.

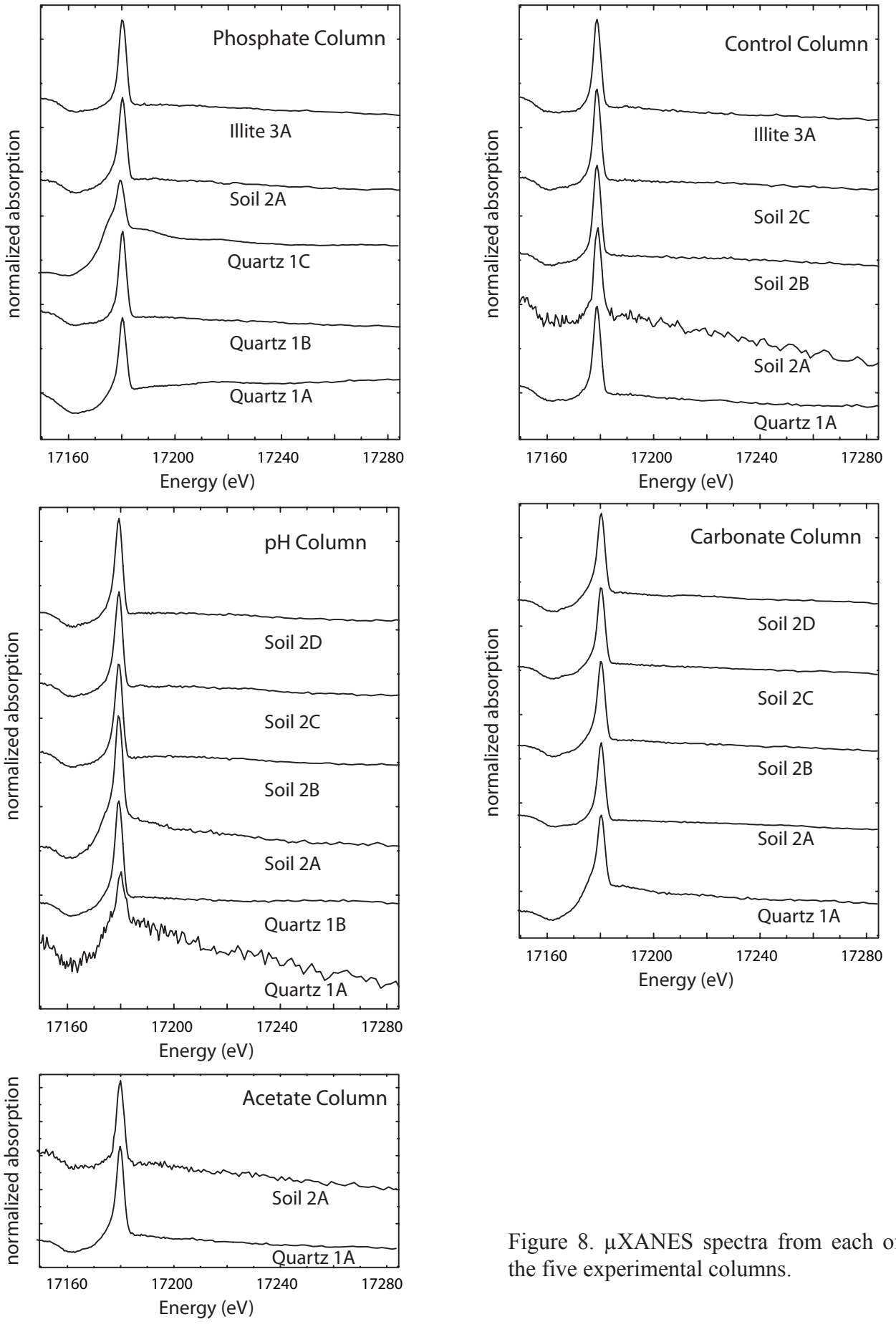

Figure 8. μXANES spectra from each of the five experimental columns.

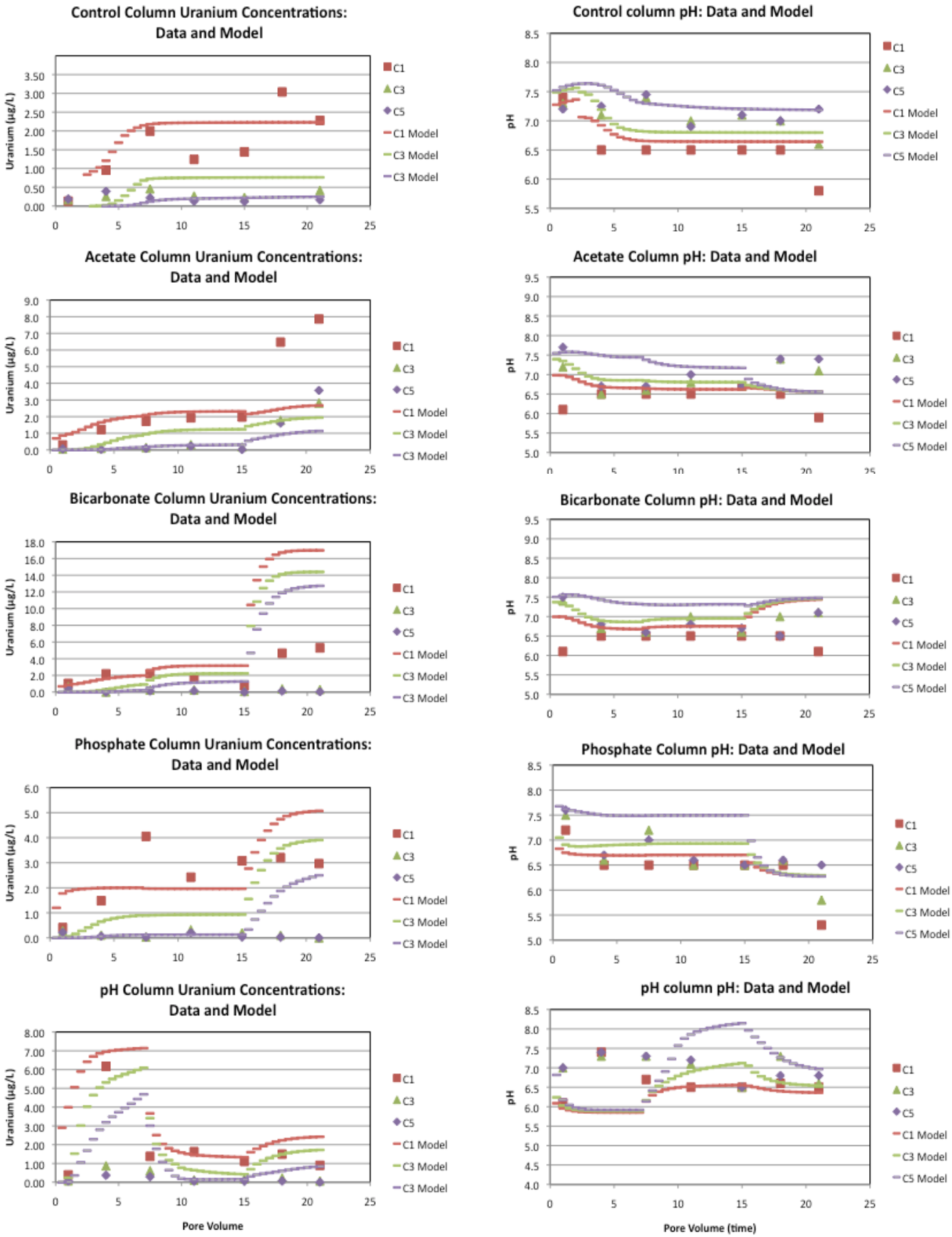

Figure 9. Results of reactive transport models using the computer code PHREEQC, with time across the X-axis presented in terms of pore volumes of fluid passed. Values represent pore water compositions. Data: symbols. Models: horizontal dash marks. Data from ports 4 and 5 not shown for clarity.

FINAL TECHNICAL REPORT
DOE/SC0001389

INVESTIGATION OF URANIUM ATTENUATION AND RELEASE AT COLUMN AND PORE SCALES IN RESPONSE TO ADVECTIVE GEOCHEMICAL GRADIENTS

Appendix A: Geochemical Model Files

DOE/SC0001389 Final technical report: Investigation of uranium attenuation and release at column and pore scales in response to advective geochemical gradients

Control column model

Input file: a_ornl_con17
Output file: a_ornl_con17.out
Database file: database/wateq4f_testU.dat

```
------------------
    SOLUTION_MASTER_SPECIES
    SOLUTION_SPECIES
    PHASES
    EXCHANGE_MASTER_SPECIES
    EXCHANGE_SPECIES
    SURFACE_MASTER_SPECIES
    SURFACE_SPECIES
    RATES
    END
------------------
    TITLE Sorption of uranium
    SURFACE_MASTER_SPECIES
        Si_ Si_OH   #Quartz
        Soilx_w Soilx_wOH #Soil weak site (KSS adaptation)
        Soilx_s Soilx_sOH #Soil strong site (KSS adaptation)
        Al_ Al_OH #clay
        Hfo_w Hfo_wOH
        Hfo_s  Hfo_sOH
    SURFACE_SPECIES
        Si_OH = Si_OH
        log_k 0.0
        Si_OH = Si_O- + H+
        log_k -7.6              #Korichi 2009 log K = -7.06
        Si_OH + H+ = Si_OH2+
        log_k -1.24
        Si_OH + UO2+2 = Si_OUO2+ + H+
        log_k -0.30             #Korici 2009 log K = 0.146
        Si_OH + UO2+2 + 3H2O = Si_OUO2(OH)3-2 + 4H+
        log_k -18.7
        Soilx_wOH = Soilx_wOH
        log_k 0.0
        Soilx_wOH + UO2+2  =  Soilx_wOUO2+ + H+
        log_K      3.52
        Soilx_wOH + UO2+2 + 2CO3-2  =  Soilx_wOUO2(CO3)2-3  +  H+
        log_K      13.336
        Soilx_sOH = Soilx_sOH
        log_k 0.0
        Soilx_sOH + UO2+2  =  Soilx_sOUO2+ + H+
        log_K      7.91
        Soilx_sOH + UO2+2 + 2CO3-2  =  Soilx_sOUO2(CO3)2-3  +  H+
        log_K      18.176
        Al_OH=Al_OH
        log_k 0.0
        Si_OH + 3UO2+2 + 5H2O = Si_O(UO2)3(OH)5 + 6H+
        log_k -16.8
        Al_OH + H+ = Al_OH2+
```

```
    log_k 7.6
    Al_OH = Al_O-+ H+
    log_k -10.6
    Al_OH + UO2+2 = Al_OUO2+ + H+
    log_k 2.47
    Al_OH + 3UO2+2 + 5H2O = Al_O(UO2)3(OH)5 + 6H+
    log_k -17.7
    Hfo_wOH=Hfo_wOH
    log_k 0.0
    Hfo_sOH=Hfo_sOH
    log_k 0.0
    Hfo_wOH + H+ =Hfo_wOH2+
    log_k 7.29
    Hfo_sOH + H+ = Hfo_sOH2+
    log_k 7.29
    Hfo_wOH = Hfo_wO-+ H+
    log_k -8.93
    Hfo_sOH = Hfo_sO-+ H+
    log_k -8.93
    Hfo_wOH + CO3-2 + H+ = Hfo_wOCO2-+ H2O
    log_k 12.78
    Hfo_sOH + CO3-2+ H+ = Hfo_sOCO2-+ H2O
    log_k 12.78
    Hfo_wOH + CO3-2+ 2H+ = Hfo_wOCO2H + H2O
    log_k 20.37
    Hfo_sOH + CO3-2+ 2H+ =Hfo_sOCO2H + H2O
    log_k 20.37
    2Hfo_wOH + UO2+2 = (Hfo_wO)2UO2 + 2H+
    log_k -6.06
    2Hfo_sOH + UO2+2 =(Hfo_sO)2UO2 + 2H+
    log_k -2.35
    2Hfo_wOH + UO2+2+ CO3-2 =(Hfo_wO)2UO2CO3-2+ 2H+
    log_k -0.24
    2Hfo_sOH + UO2+2+ CO3-2 =(Hfo_sO)2UO2CO3-2+ 2H+
    log_k 4.33
SURFACE 1 #Quartz Surface
    Si_OH   2E-4    0.5     25
SAVE SURFACE 1
SURFACE 2 #Quartz Surface
    Si_OH   2E-4    0.5     25
SAVE SURFACE 2
SURFACE 3 # Soil surface, need to assess Tx & Sx parameters
    Si_OH   1E-3    0.5     45
    Al_OH   1E-3        20  6
    Hfo_wOH 1E-03   200     0.155
    Hfo_sOH 1E-04                   #assumes 10 weak sites per strong site
SAVE SURFACE 3
SURFACE 4 #Quartz Surface
    Si_OH   1.72E-4     0.5     45
SAVE SURFACE 4
SURFACE 5 # Clay/Quartz mixture 4 quartz: 1 illite
    Si_OH   1E-4     0.5    24
    Al_OH   4E-4    20  6
SAVE SURFACE 5
SURFACE 6 #Quartz Surface
    Si_OH   1.72E-4     0.5     45
SAVE SURFACE 6
```

```
SURFACE 7 # Quartz + Goethite
    Si_OH   1.53E-03     0.5    28
    Hfo_wOH 3.1E-04     200     0.155
    Hfo_sOH 3.1E-06                 #assumes 100 weak sites per strong site
SAVE SURFACE 7
SURFACE 8 #Quartz Surface
    Si_OH   1.72E-4     0.5     45
SAVE SURFACE 8
SURFACE 9 # Soil surface
    Si_OH   1E-3    0.5     45
    Al_OH   1E-4        20  6
    Hfo_wOH 1E-03   200     0.155
    Hfo_sOH 1E-05                   #assumes 100 weak sites per strong site
SAVE SURFACE 9
SURFACE 10 #Quartz Surface
    Si_OH   1.72E-4     0.5     45
SAVE SURFACE 10
EQUILIBRIUM_PHASES 1    #PLAY SAND, CELL 1A
    Quartz
    K-Feldspar
    B-UO2(OH)2  0 0     # THIS LOOKS PRETTY GOOD.
    Schoepite .1 0  # U too low.
SAVE EQUILIBRIUM_PHASES 1
EQUILIBRIUM_PHASES 2    #PLAY SAND, CELL 1B
    Quartz
    K-Feldspar
    B-UO2(OH)2  0 0
    Schoepite .1 0
SAVE EQUILIBRIUM_PHASES 2
EQUILIBRIUM_PHASES 3    #SOIL, CELL 2
    Quartz
    B-UO2(OH)2  0 0
    Schoepite 0 0
SAVE EQUILIBRIUM_PHASES 3
EQUILIBRIUM_PHASES 4    #PLAY SAND, CELL 3
    Quartz
    K-Feldspar
    B-UO2(OH)2  0 0
    Schoepite 0 0
SAVE EQUILIBRIUM_PHASES 4
EQUILIBRIUM_PHASES 5    #QUARTZ + ILLITE, CELL 4
    Quartz
    Illite 2.8 1
    B-UO2(OH)2  0 0
    Schoepite 0 0
SAVE EQUILIBRIUM_PHASES 5
EQUILIBRIUM_PHASES 6    #PLAY SAND, CELL 5
    Quartz
    B-UO2(OH)2  0 0
    Schoepite 0 0
SAVE EQUILIBRIUM_PHASES 6
EQUILIBRIUM_PHASES 7    #QUARTZ + GOETHITE, CELL 6
    Quartz
    Goethite
    B-UO2(OH)2  0 0
    Schoepite 0 0
SAVE EQUILIBRIUM_PHASES 7
```

```
    EQUILIBRIUM_PHASES 8    #PLAY SAND, CELL 7
        Quartz
        B-UO2(OH)2  0 0
        Schoepite 0 0
    SAVE EQUILIBRIUM_PHASES 8
    EQUILIBRIUM_PHASES 9    #SOIL, CELL 8
        Quartz
        B-UO2(OH)2  0 0
        Schoepite 0 0
    SAVE EQUILIBRIUM_PHASES 9
    EQUILIBRIUM_PHASES 10   #PLAY SAND, CELL 9
        Quartz
        B-UO2(OH)2  0 0
        Schoepite 0 0
    SAVE EQUILIBRIUM_PHASES 10
    USER_PUNCH
        heading U(ppm)
        10  REM convert to ppm
        20  PUNCH TOT("U")*238*1000
        end
    END
------------------
    SELECTED_OUTPUT
        reset true
        file a_ornl_con17.sel
        user_punch true
        ph true
        pe false
        reaction false
        temperature false
        alkalinity false
        ionic_strength false
        water false
        charge_balance false
        percent_error false
        totals U K Fe C #Si Na
        molalities
            UO2+2
            Si_OUO2+
            Si_OUO2(OH)3-2
            Si_O(UO2)3(OH)5
            Soilx_wOUO2+
            Soilx_sOUO2+
            Soilx_wOUO2(CO3)2-3
            Soilx_sOUO2(CO3)2-3
            Al_OUO2+
            Al_O(UO2)3(OH)5
            (Hfo_wO)2UO2
            (Hfo_sO)2UO2
            (Hfo_wO)2UO2CO3-2
            (Hfo_sO)2UO2CO3-2
        si
            Quartz
            K-feldspar
            Illite
            UO2(OH)2(beta)      #llnl
            CaUO4               #llnl
```

```
            UO3:.9H2O(alpha)    #llnl
            B-UO2(OH)2
            Becquerelite
            Clarkeite
            Compreignacite
            Schoepite
            Soddyite
            Uraninite(c)
            Uranophane
            CO2(g)
        equilibrium_phases
            B-UO2(OH)2
            Becquerelite
            Clarkeite
            Compreignacite
            Schoepite
            Soddyite
            Uraninite(c)
            Uranophane
    END
------------------
    SOLUTION 0-10 background ORNL GW
        pH      7.2
        units mmol/L
        Mg      1.10
        S(6)    0.66
        Ca      3.34
        N(+5)   6.68 charge
        K       0.14
        Na      1.29
        Cl      2.31
    EQUILIBRIUM_PHASES
        O2(g)   -0.7
        CO2(g)  -6.5
    PRINT
          selected_output false
    END
------------------
TRANSPORT
        -cells                10
        -shifts               10
        -lengths              .01 .01 .02
        -time_step            8640
        -flow_direction       forward
        -boundary_condition   flux flux
        -dispersivity         0.08
        -correct_disp         true
        -diffusion_coef       0.3e-9
        -print_cells          1-10
        -print_frequency      1
        -punch_cells          1-10
        -punch_frequency      5
PRINT
      -selected_output true
END
------------------
SOLUTION 0 background ORNL GW + U
```

```
    pH      6.8
    -units mmol/L
    Mg      1.10
    S(6)    0.66
    Ca      3.34
    N(+5)   6.68 charge
    K       0.14
    Na      1.29
    Cl      2.31
    U(6)    0.1
EQUILIBRIUM_PHASES
    O2(g)   -0.7
    CO2(g)  -6.5
SAVE SOLUTION 0
PRINT
      -selected_output false
END
------------------
TRANSPORT
        -shifts               190          # unitless time steps, PV = shift/cells
PRINT
      -selected_output true
END
------------------
```

DOE/SC0001389 Final technical report: Investigation of uranium attenuation and release at column and pore scales in response to advective geochemical gradients

Acetate column model

Input file: a_ornl_ace6
Output file: a_ornl_ace6.out
Database file: database/wateq4f_testU.dat

```
------------------
    SOLUTION_MASTER_SPECIES
    SOLUTION_SPECIES
    PHASES
    EXCHANGE_MASTER_SPECIES
    EXCHANGE_SPECIES
    SURFACE_MASTER_SPECIES
    SURFACE_SPECIES
    RATES
    END
------------------
    TITLE Sorption of uranium
    SURFACE_MASTER_SPECIES
        Si_ Si_OH   #Quartz
        Soilx_w Soilx_wOH #Soil weak site (KSS adaptation)
        Soilx_s Soilx_sOH #Soil strong site (KSS adaptation)
        Al_ Al_OH #clay
        Hfo_w Hfo_wOH
        Hfo_s  Hfo_sOH
    SURFACE_SPECIES
        Si_OH = Si_OH
        log_k 0.0
        Si_OH = Si_O- + H+
        log_k -7.6              #Korichi 2009 log K = -7.06
        Si_OH + H+ = Si_OH2+
        log_k -1.24
        Si_OH + UO2+2 = Si_OUO2+ + H+
        log_k -0.30             #Korici 2009 log K = 0.146
        Si_OH + UO2+2 + 3H2O = Si_OUO2(OH)3-2 + 4H+
        log_k -18.7
        Soilx_wOH = Soilx_wOH
        log_k 0.0
        Soilx_wOH + UO2+2  =  Soilx_wOUO2+ + H+
        log_K      3.52
        Soilx_wOH + UO2+2 + 2CO3-2  =  Soilx_wOUO2(CO3)2-3  +  H+
        log_K      13.336
        Soilx_sOH = Soilx_sOH
        log_k 0.0
        Soilx_sOH + UO2+2  =  Soilx_sOUO2+ + H+
        log_K      7.91
        Soilx_sOH + UO2+2 + 2CO3-2  =  Soilx_sOUO2(CO3)2-3  +  H+
        log_K      18.176
        Al_OH=Al_OH
        log_k 0.0
        Si_OH + 3UO2+2 + 5H2O = Si_O(UO2)3(OH)5 + 6H+
        log_k -16.8
        Al_OH + H+ = Al_OH2+
        log_k 7.6
        Al_OH = Al_O-+ H+
```

```
    log_k -10.6
    Al_OH + UO2+2 = Al_OUO2+ + H+
    log_k 2.47
    Al_OH + 3UO2+2 + 5H2O = Al_O(UO2)3(OH)5 + 6H+
    log_k -17.7
    Hfo_wOH=Hfo_wOH
    log_k 0.0
    Hfo_sOH=Hfo_sOH
    log_k 0.0
    Hfo_wOH + H+ =Hfo_wOH2+
    log_k 7.29
    Hfo_sOH + H+ = Hfo_sOH2+
    log_k 7.29
    Hfo_wOH = Hfo_wO-+ H+
    log_k -8.93
    Hfo_sOH = Hfo_sO-+ H+
    log_k -8.93
    Hfo_wOH + CO3-2 + H+ = Hfo_wOCO2-+ H2O
    log_k 12.78
    Hfo_sOH + CO3-2+ H+ = Hfo_sOCO2-+ H2O
    log_k 12.78
    Hfo_wOH + CO3-2+ 2H+ = Hfo_wOCO2H + H2O
    log_k 20.37
    Hfo_sOH + CO3-2+ 2H+ =Hfo_sOCO2H + H2O
    log_k 20.37
    2Hfo_wOH + UO2+2 = (Hfo_wO)2UO2 + 2H+
    log_k -6.06
    2Hfo_sOH + UO2+2 =(Hfo_sO)2UO2 + 2H+
    log_k -2.35
    2Hfo_wOH + UO2+2+ CO3-2 =(Hfo_wO)2UO2CO3-2+ 2H+
    log_k -0.24
    2Hfo_sOH + UO2+2+ CO3-2 =(Hfo_sO)2UO2CO3-2+ 2H+
    log_k 4.33
SURFACE 1 #Quartz Surface
    Si_OH   2E-4    0.5     25
SAVE SURFACE 1
SURFACE 2 #Quartz Surface
    Si_OH   2E-4    0.5     25
SAVE SURFACE 2
SURFACE 3 # Soil surface, need to assess Tx & Sx parameters
    Si_OH   1E-3    0.5     45
    Al_OH   1E-3        20  6
    Hfo_wOH 1E-03   200     0.155
    Hfo_sOH 1E-04                   #assumes 10 weak sites per strong site
SAVE SURFACE 3
SURFACE 4 #Quartz Surface
    Si_OH   1.72E-4     0.5     45
SAVE SURFACE 4
SURFACE 5 # Clay/Quartz mixture 4 quartz: 1 illite
    Si_OH   1E-4     0.5    24
    Al_OH   4E-4    20  6
SAVE SURFACE 5
SURFACE 6 #Quartz Surface
    Si_OH   1.72E-4     0.5     45
SAVE SURFACE 6
SURFACE 7 # Quartz + Goethite
    Si_OH   1.53E-03     0.5    28
```

```
    Hfo_wOH 3.1E-04     200     0.155
    Hfo_sOH 3.1E-06                 #assumes 100 weak sites per strong site
SAVE SURFACE 7
SURFACE 8 #Quartz Surface
    Si_OH   1.72E-4     0.5     45
SAVE SURFACE 8
SURFACE 9 # Soil surface
    Si_OH   1E-3    0.5     45
    Al_OH   1E-4        20  6
    Hfo_wOH 1E-03   200     0.155
    Hfo_sOH 1E-05                   #assumes 100 weak sites per strong site
SAVE SURFACE 9
SURFACE 10 #Quartz Surface
    Si_OH   1.72E-4     0.5     45
SAVE SURFACE 10
EQUILIBRIUM_PHASES 1    #PLAY SAND, CELL 1A
    Quartz
    K-Feldspar
    B-UO2(OH)2  0 0     # THIS LOOKS PRETTY GOOD.
    Schoepite .1 0  # U too low.
SAVE EQUILIBRIUM_PHASES 1
EQUILIBRIUM_PHASES 2    #PLAY SAND, CELL 1B
    Quartz
    K-Feldspar
    B-UO2(OH)2  0 0
    Schoepite .1 0
SAVE EQUILIBRIUM_PHASES 2
EQUILIBRIUM_PHASES 3    #SOIL, CELL 2
    Quartz
    B-UO2(OH)2  0 0
    Schoepite .1 0
SAVE EQUILIBRIUM_PHASES 3
EQUILIBRIUM_PHASES 4    #PLAY SAND, CELL 3
    Quartz
    K-Feldspar
    B-UO2(OH)2  0 0
    Schoepite .1 0
SAVE EQUILIBRIUM_PHASES 4
EQUILIBRIUM_PHASES 5    #QUARTZ + ILLITE, CELL 4
    Quartz
    Illite 2.8 1
    B-UO2(OH)2  0 0
    Schoepite 0 0
SAVE EQUILIBRIUM_PHASES 5
EQUILIBRIUM_PHASES 6    #PLAY SAND, CELL 5
    Quartz
    K-Feldspar
    B-UO2(OH)2  0 0
    Schoepite .1 0
SAVE EQUILIBRIUM_PHASES 6
EQUILIBRIUM_PHASES 7    #QUARTZ + GOETHITE, CELL 6
    Quartz
    Goethite
    B-UO2(OH)2  0 0
    Schoepite .1 0
SAVE EQUILIBRIUM_PHASES 7
EQUILIBRIUM_PHASES 8    #PLAY SAND, CELL 7
```

```
        Quartz
        K-Feldspar
        B-UO2(OH)2  0 0
        Schoepite .1 0
    SAVE EQUILIBRIUM_PHASES 8
    EQUILIBRIUM_PHASES 9    #SOIL, CELL 8
        Quartz
        B-UO2(OH)2  0 0
        Schoepite .1 0
    SAVE EQUILIBRIUM_PHASES 9
    EQUILIBRIUM_PHASES 10   #PLAY SAND, CELL 9
        Quartz
        K-Feldspar
        B-UO2(OH)2  0 0
        Schoepite .1 0
    SAVE EQUILIBRIUM_PHASES 10
    USER_PUNCH
        heading U(ppm)
        10  REM convert to ppm
        20  PUNCH TOT("U")*238*1000
        end
    END
------------------
    SELECTED_OUTPUT
        reset true
        file a_ornl_ace6.sel
        user_punch true
        ph true
        pe false
        reaction false
        temperature false
        alkalinity false
        ionic_strength false
        water false
        charge_balance false
        percent_error false
        totals U K Fe C #Si Na
        molalities
            UO2+2
            Si_OUO2+
            Si_OUO2(OH)3-2
            Si_O(UO2)3(OH)5
            Soilx_wOUO2+
            Soilx_sOUO2+
            Soilx_wOUO2(CO3)2-3
            Soilx_sOUO2(CO3)2-3
            Al_OUO2+
            Al_O(UO2)3(OH)5
            (Hfo_wO)2UO2
            (Hfo_sO)2UO2
            (Hfo_wO)2UO2CO3-2
            (Hfo_sO)2UO2CO3-2
        si
            Quartz
            K-feldspar
            Illite
            UO2(OH)2(beta)      #llnl
```

```
            CaUO4               #llnl
            UO3:.9H2O(alpha)    #llnl
            B-UO2(OH)2
            Becquerelite
            Clarkeite
            Compreignacite
            Schoepite
            Soddyite
            Uraninite(c)
            Uranophane
            CO2(g)
        equilibrium_phases
            B-UO2(OH)2
            Becquerelite
            Clarkeite
            Compreignacite
            Schoepite
            Soddyite
            Uraninite(c)
            Uranophane
    END
------------------
    SOLUTION 1-10 background ORNL GW
        pH      7.2
        units mmol/L
        Mg      1.10
        S(6)    0.66
        Ca      3.34
        N(+5)   6.68 charge
        K       0.14
        Na      1.29
        Cl      2.31
    EQUILIBRIUM_PHASES 100
        O2(g)   -0.7
        CO2(g)  -6.5
    END
------------------
SOLUTION 0 background ORNL GW + U + Ac1
    pH      7.4
    -units mmol/L
    Mg      1.10
    S(6)    0.66
    Ca      3.34
    N(+5)   6.68
    K       0.16
    Na      1.29
    Cl      2.31 charge
    U(6)    0.1
    Ac      0.01
EQUILIBRIUM_PHASES 10
    O2(g)   -0.7
    CO2(g)  -6.5
SAVE SOLUTION 0
PRINT
      -selected_output false
END
------------------
```

```
TRANSPORT
        -cells                10
        -shifts               10
        -lengths              .01 .01 .02
        -time_step            8640
        -flow_direction       forward
        -boundary_condition   flux flux
        -dispersivity         0.08
        -correct_disp         true
        -diffusion_coef       0.3e-9
        -print_cells          1-10
        -print_frequency      1
        -punch_cells          1-10
        -punch_frequency      5
PRINT
      -selected_output true
END
------------------
TRANSPORT
        -shifts               60          # unitless time steps, PV = shift/cells
PRINT
      -selected_output true
END
------------------
SOLUTION 0 background ORNL GW + U + Ac2
    pH      7.4
    -units mmol/L
    Mg      1.10
    S(6)    0.66
    Ca      3.34
    N(+5)   6.68
    K       0.24
    Na      1.29
    Cl      2.31 charge
    U(6)    0.1
    Ac      0.1
EQUILIBRIUM_PHASES 10
    O2(g)   -0.7
    CO2(g)  -6.5
SAVE SOLUTION 0
PRINT
      -selected_output false
END
------------------
TRANSPORT
        -shifts               80          # unitless time steps, PV = shift/cells
PRINT
      -selected_output true
END
------------------
SOLUTION 0 background ORNL GW + U + Ac3
    pH      7.4
    -units mmol/L
    Mg      1.10
    S(6)    0.66
    Ca      3.34
    N(+5)   6.68
```

```
    K       1.14
    Na      1.29
    Cl      2.31 charge
    U(6)    0.1
    Ac      1
EQUILIBRIUM_PHASES 10
    O2(g)   -0.7
    CO2(g)  -6.5
SAVE SOLUTION 0
PRINT
      -selected_output false
END
------------------
TRANSPORT
        -shifts               60          # unitless time steps, PV = shift/cells
PRINT
      -selected_output true
END
------------------
```

DOE/SC0001389 Final technical report: Investigation of uranium attenuation and release at column and pore scales in response to advective geochemical gradients

Bicarbonate column model

```
   Input file: a_ornl_bic4
  Output file: a_ornl_bic4.out
Database file: database/wateq4f_testU.dat
------------------
    SOLUTION_MASTER_SPECIES
    SOLUTION_SPECIES
    PHASES
    EXCHANGE_MASTER_SPECIES
    EXCHANGE_SPECIES
    SURFACE_MASTER_SPECIES
    SURFACE_SPECIES
    RATES
    END
------------------
    TITLE Sorption of uranium
    SURFACE_MASTER_SPECIES
        Si_ Si_OH   #Quartz
        Soilx_w Soilx_wOH #Soil weak site (KSS adaptation)
        Soilx_s Soilx_sOH #Soil strong site (KSS adaptation)
        Al_ Al_OH #clay
        Hfo_w Hfo_wOH
        Hfo_s  Hfo_sOH
    SURFACE_SPECIES
        Si_OH = Si_OH
        log_k 0.0
        Si_OH = Si_O- + H+
        log_k -7.6              #Korichi 2009 log K = -7.06
        Si_OH + H+ = Si_OH2+
        log_k -1.24
        Si_OH + UO2+2 = Si_OUO2+ + H+
        log_k -0.30             #Korici 2009 log K = 0.146
        Si_OH + UO2+2 + 3H2O = Si_OUO2(OH)3-2 + 4H+
        log_k -18.7
        Soilx_wOH = Soilx_wOH
        log_k 0.0
        Soilx_wOH + UO2+2  =  Soilx_wOUO2+ + H+
        log_K      3.52
        Soilx_wOH + UO2+2 + 2CO3-2  =  Soilx_wOUO2(CO3)2-3  +  H+
        log_K      13.336
        Soilx_sOH = Soilx_sOH
        log_k 0.0
        Soilx_sOH + UO2+2  =  Soilx_sOUO2+ + H+
        log_K      7.91
        Soilx_sOH + UO2+2 + 2CO3-2  =  Soilx_sOUO2(CO3)2-3  +  H+
        log_K      18.176
        Al_OH=Al_OH
        log_k 0.0
        Si_OH + 3UO2+2 + 5H2O = Si_O(UO2)3(OH)5 + 6H+
        log_k -16.8
        Al_OH + H+ = Al_OH2+
        log_k 7.6
        Al_OH = Al_O-+ H+
```

```
    log_k -10.6
    Al_OH + UO2+2 = Al_OUO2+ + H+
    log_k 2.47
    Al_OH + 3UO2+2 + 5H2O = Al_O(UO2)3(OH)5 + 6H+
    log_k -17.7
    Hfo_wOH=Hfo_wOH
    log_k 0.0
    Hfo_sOH=Hfo_sOH
    log_k 0.0
    Hfo_wOH + H+ =Hfo_wOH2+
    log_k 7.29
    Hfo_sOH + H+ = Hfo_sOH2+
    log_k 7.29
    Hfo_wOH = Hfo_wO-+ H+
    log_k -8.93
    Hfo_sOH = Hfo_sO-+ H+
    log_k -8.93
    Hfo_wOH + CO3-2 + H+ = Hfo_wOCO2-+ H2O
    log_k 12.78
    Hfo_sOH + CO3-2+ H+ = Hfo_sOCO2-+ H2O
    log_k 12.78
    Hfo_wOH + CO3-2+ 2H+ = Hfo_wOCO2H + H2O
    log_k 20.37
    Hfo_sOH + CO3-2+ 2H+ =Hfo_sOCO2H + H2O
    log_k 20.37
    2Hfo_wOH + UO2+2 = (Hfo_wO)2UO2 + 2H+
    log_k -6.06
    2Hfo_sOH + UO2+2 =(Hfo_sO)2UO2 + 2H+
    log_k -2.35
    2Hfo_wOH + UO2+2+ CO3-2 =(Hfo_wO)2UO2CO3-2+ 2H+
    log_k -0.24
    2Hfo_sOH + UO2+2+ CO3-2 =(Hfo_sO)2UO2CO3-2+ 2H+
    log_k 4.33
SURFACE 1 #Quartz Surface
    Si_OH   2E-4    0.5     25
SAVE SURFACE 1
SURFACE 2 #Quartz Surface
    Si_OH   2E-4    0.5     25
SAVE SURFACE 2
SURFACE 3 # Soil surface, need to assess Tx & Sx parameters
    Si_OH   1E-3    0.5     45
    Al_OH   1E-3        20  6
    Hfo_wOH 1E-03   200     0.155
    Hfo_sOH 1E-04                   #assumes 10 weak sites per strong site
SAVE SURFACE 3
SURFACE 4 #Quartz Surface
    Si_OH   1.72E-4     0.5     45
SAVE SURFACE 4
SURFACE 5 # Clay/Quartz mixture 4 quartz: 1 illite
    Si_OH   1E-4     0.5    24
    Al_OH   4E-4    20  6
SAVE SURFACE 5
SURFACE 6 #Quartz Surface
    Si_OH   1.72E-4     0.5     45
SAVE SURFACE 6
SURFACE 7 # Quartz + Goethite
    Si_OH   1.53E-03     0.5    28
```

```
    Hfo_wOH 3.1E-04     200     0.155
    Hfo_sOH 3.1E-06                 #assumes 100 weak sites per strong site
SAVE SURFACE 7
SURFACE 8 #Quartz Surface
    Si_OH   1.72E-4     0.5     45
SAVE SURFACE 8
SURFACE 9 # Soil surface
    Si_OH   1E-3    0.5     45
    Al_OH   1E-4        20  6
    Hfo_wOH 1E-03   200     0.155
    Hfo_sOH 1E-05                   #assumes 100 weak sites per strong site
SAVE SURFACE 9
SURFACE 10 #Quartz Surface
    Si_OH   1.72E-4     0.5     45
SAVE SURFACE 10
EQUILIBRIUM_PHASES 1    #PLAY SAND, CELL 1A
    Quartz
    K-Feldspar
    B-UO2(OH)2  0 0     # THIS LOOKS PRETTY GOOD.
    Schoepite .1 0  # U too low.
SAVE EQUILIBRIUM_PHASES 1
EQUILIBRIUM_PHASES 2    #PLAY SAND, CELL 1B
    Quartz
    K-Feldspar
    B-UO2(OH)2  0 0
    Schoepite .1 0
SAVE EQUILIBRIUM_PHASES 2
EQUILIBRIUM_PHASES 3    #SOIL, CELL 2
    Quartz
    B-UO2(OH)2  0 0
    Schoepite .1 0
SAVE EQUILIBRIUM_PHASES 3
EQUILIBRIUM_PHASES 4    #PLAY SAND, CELL 3
    Quartz
    K-Feldspar
    B-UO2(OH)2  0 0
    Schoepite .1 0
SAVE EQUILIBRIUM_PHASES 4
EQUILIBRIUM_PHASES 5    #QUARTZ + ILLITE, CELL 4
    Quartz
    Illite 2.8 1
    B-UO2(OH)2  0 0
    Schoepite 0 0
SAVE EQUILIBRIUM_PHASES 5
EQUILIBRIUM_PHASES 6    #PLAY SAND, CELL 5
    Quartz
    B-UO2(OH)2  0 0
    Schoepite .1 0
SAVE EQUILIBRIUM_PHASES 6
EQUILIBRIUM_PHASES 7    #QUARTZ + GOETHITE, CELL 6
    Quartz
    Goethite
    B-UO2(OH)2  0 0
    Schoepite .1 0
SAVE EQUILIBRIUM_PHASES 7
EQUILIBRIUM_PHASES 8    #PLAY SAND, CELL 7
    Quartz
```

```
        B-UO2(OH)2  0 0
        Schoepite .1 0
    SAVE EQUILIBRIUM_PHASES 8
    EQUILIBRIUM_PHASES 9    #SOIL, CELL 8
        Quartz
        B-UO2(OH)2  0 0
        Schoepite .1 0
    SAVE EQUILIBRIUM_PHASES 9
    EQUILIBRIUM_PHASES 10   #PLAY SAND, CELL 9
        Quartz
        B-UO2(OH)2  0 0
        Schoepite .1 0
    SAVE EQUILIBRIUM_PHASES 10
    USER_PUNCH
        heading U(ppm)
        10  REM convert to ppm
        20  PUNCH TOT("U")*238*1000
        end
    END
-----------------------------------
    SELECTED_OUTPUT
        reset true
        file a_ornl_bic4.sel
        user_punch true
        ph true
        pe false
        reaction false
        temperature false
        alkalinity false
        ionic_strength false
        water false
        charge_balance false
        percent_error false
        totals U K Fe C #Si Na
        molalities
            UO2+2
            Si_OUO2+
            Si_OUO2(OH)3-2
            Si_O(UO2)3(OH)5
            Soilx_wOUO2+
            Soilx_sOUO2+
            Soilx_wOUO2(CO3)2-3
            Soilx_sOUO2(CO3)2-3
            Al_OUO2+
            Al_O(UO2)3(OH)5
            (Hfo_wO)2UO2
            (Hfo_sO)2UO2
            (Hfo_wO)2UO2CO3-2
            (Hfo_sO)2UO2CO3-2
        si
            Quartz
            K-feldspar
            Illite
            UO2(OH)2(beta)      #llnl
            CaUO4               #llnl
            UO3:.9H2O(alpha)    #llnl
            B-UO2(OH)2
```

```
            Becquerelite
            Clarkeite
            Compreignacite
            Schoepite
            Soddyite
            Uraninite(c)
            Uranophane
            CO2(g)
        equilibrium_phases
            B-UO2(OH)2
            Becquerelite
            Clarkeite
            Compreignacite
            Schoepite
            Soddyite
            Uraninite(c)
            Uranophane
    END
------------------
    USER_PUNCH
        heading U(ppm)
        10  REM convert to ppm
        20  PUNCH TOT("U")*238*1000
        end
    END
------------------
    SOLUTION 1-10 background ORNL GW
        pH      7.4
        units mmol/L
        Mg      1.10
        S(6)    0.66
        Ca      3.34
        N(+5)   6.68
        K       0.14
        Na      1.29
        Cl      2.31
    EQUILIBRIUM_PHASES 10
        O2(g)   -0.7
    PRINT
          selected_output false
    END
------------------
SOLUTION 0 background ORNL GW + U + Bic1
    pH      7.4
    -units mmol/L
    Mg      1.10
    S(6)    0.66
    Ca      3.34
    N(+5)   6.68
    K       0.14
    Na      1.29
    Cl      2.31 charge
    U(6)    0.1
    C(+4)   0.001
EQUILIBRIUM_PHASES 10
    O2(g)   -0.7
SAVE SOLUTION 0
```

```
PRINT
      -selected_output false
END
------------------
TRANSPORT
        -cells                10
        -shifts               10
        -lengths              .01 .01 .02
        -time_step            8640
        -flow_direction       forward
        -boundary_condition   flux flux
        -dispersivity         0.08
        -correct_disp         true
        -diffusion_coef       0.3e-9
        -print_cells          1-10
        -print_frequency      1
        -punch_cells          1-10
        -punch_frequency      5
PRINT
      -selected_output true
END
------------------
TRANSPORT
        -shifts               60          # unitless time steps, PV = shift/cells
PRINT
      -selected_output true
END
------------------
SOLUTION 0 background ORNL GW + U + Bic2
    pH      7.4
    -units mmol/L
    Mg      1.10
    S(6)    0.66
    Ca      3.34
    N(+5)   6.68
    K       0.16
    Na      1.29
    Cl      2.31 charge
    U(6)    0.1
    C(+4)   0.01
EQUILIBRIUM_PHASES 10
    O2(g)   -0.7
SAVE SOLUTION 0
PRINT
      -selected_output false
END
------------------
TRANSPORT
        -shifts               80          # unitless time steps, PV = shift/cells
PRINT
      -selected_output true
END
------------------
SOLUTION 0 background ORNL GW + U + Bic3
    pH      7.4
    -units mmol/L
    Mg      1.10
```

```
    S(6)    0.66
    Ca      3.34
    N(+5)   6.68
    K       0.24
    Na      1.29
    Cl      2.31 charge
    U(6)    0.1
    C(+4)   0.1
EQUILIBRIUM_PHASES 10
    O2(g)   -0.7
SAVE SOLUTION 0
PRINT
      -selected_output false
END
------------------
TRANSPORT
        -shifts               60          # unitless time steps, PV = shift/cells
PRINT
      -selected_output true
END
------------------
```

DOE/SC0001389 Final technical report: Investigation of uranium attenuation and release at column and pore scales in response to advective geochemical gradients

Phosphate column model

```
   Input file: a_ornl_phos9
  Output file: a_ornl_phos9.out
Database file: database/wateq4f_testU.dat

------------------
    SOLUTION_MASTER_SPECIES
    SOLUTION_SPECIES
    PHASES
    EXCHANGE_MASTER_SPECIES
    EXCHANGE_SPECIES
    SURFACE_MASTER_SPECIES
    SURFACE_SPECIES
    RATES
    END
------------------
    TITLE Sorption of uranium
    SURFACE_MASTER_SPECIES
        Si_ Si_OH   #Quartz
        Soilx_w Soilx_wOH #Soil weak site (KSS adaptation)
        Soilx_s Soilx_sOH #Soil strong site (KSS adaptation)
        Al_ Al_OH #clay
        Hfo_w Hfo_wOH
        Hfo_s  Hfo_sOH
        Fe_ Fe_OH
    SURFACE_SPECIES
        Si_OH = Si_OH
        log_k 0.0
        Si_OH = Si_O- + H+
        log_k -7.6              #Korichi 2009 log K = -7.06
        Si_OH + H+ = Si_OH2+
        log_k -1.24
        Si_OH + UO2+2 = Si_OUO2+ + H+
        log_k -0.30             #Korici 2009 log K = 0.146
        Si_OH + UO2+2 + 3H2O = Si_OUO2(OH)3-2 + 4H+
        log_k -18.7
        Soilx_wOH = Soilx_wOH
        log_k 0.0
        Soilx_wOH + UO2+2  =  Soilx_wOUO2+ + H+
        log_K      3.52
        Soilx_wOH + UO2+2 + 2CO3-2  =  Soilx_wOUO2(CO3)2-3  +  H+
        log_K      13.336
        Soilx_sOH = Soilx_sOH
        log_k 0.0
        Soilx_sOH + UO2+2  =  Soilx_sOUO2+ + H+
        log_K      7.91
        Soilx_sOH + UO2+2 + 2CO3-2  =  Soilx_sOUO2(CO3)2-3  +  H+
        log_K      18.176
        Al_OH=Al_OH
        log_k 0.0
        Si_OH + 3UO2+2 + 5H2O = Si_O(UO2)3(OH)5 + 6H+
        log_k -16.8
        Al_OH + H+ = Al_OH2+
```

```
    log_k 7.6
    Al_OH = Al_O-+ H+
    log_k -10.6
    Al_OH + UO2+2 = Al_OUO2+ + H+
    log_k 2.47
    Al_OH + 3UO2+2 + 5H2O = Al_O(UO2)3(OH)5 + 6H+
    log_k -17.7
    Hfo_wOH=Hfo_wOH
    log_k 0.0
    Hfo_sOH=Hfo_sOH
    log_k 0.0
    Hfo_wOH + H+ =Hfo_wOH2+
    log_k 7.29
    Hfo_sOH + H+ = Hfo_sOH2+
    log_k 7.29
    Hfo_wOH = Hfo_wO-+ H+
    log_k -8.93
    Hfo_sOH = Hfo_sO-+ H+
    log_k -8.93
    Hfo_wOH + CO3-2 + H+ = Hfo_wOCO2-+ H2O
    log_k 12.78
    Hfo_sOH + CO3-2+ H+ = Hfo_sOCO2-+ H2O
    log_k 12.78
    Hfo_wOH + CO3-2+ 2H+ = Hfo_wOCO2H + H2O
    log_k 20.37
    Hfo_sOH + CO3-2+ 2H+ =Hfo_sOCO2H + H2O
    log_k 20.37
    2Hfo_wOH + UO2+2 = (Hfo_wO)2UO2 + 2H+
    log_k -6.06
    2Hfo_sOH + UO2+2 =(Hfo_sO)2UO2 + 2H+
    log_k -2.35
    2Hfo_wOH + UO2+2+ CO3-2 =(Hfo_wO)2UO2CO3-2+ 2H+
    log_k -0.24
    2Hfo_sOH + UO2+2+ CO3-2 =(Hfo_sO)2UO2CO3-2+ 2H+
    log_k 4.33
    Fe_OH = Fe_OH
    log_k 0.0
    Fe_OH +H+ = Fe_OH2 +
    log_k 7.47
    Fe_OH =Fe_O- +H+
    log_k -9.51
    Fe_OH +H2PO4- +H+ =Fe_PO4H2 +H2O
    log_k 12.68
    Fe_OH + H2PO4- = Fe_PO4H- +H2O
    log_k 7.93
    Fe_OH +H2PO4- = Fe_PO4-2 +H+ +H2O
    log_k 2.16
    2Fe_OH +UO2+2 =(Fe_O)2UO2 + 2H+
    log_k -4.66
    Fe_OH + UO2+2 + H2PO4- = Fe_PO4UO2 + H2O +H+
    log_k 10.6
SURFACE 1 #Quartz Surface
    Si_OH   2E-4    0.5     25
SAVE SURFACE 1
SURFACE 2 #Quartz Surface
    Si_OH   2E-4    0.5     25
SAVE SURFACE 2
```

```
SURFACE 3 # Soil surface, need to assess Tx & Sx parameters
    Si_OH   1E-3    0.5     45
    Al_OH   1E-3    20  6
    Fe_OH 1E-03   200    0.155
SAVE SURFACE 3
SURFACE 4 #Quartz Surface
    Si_OH   1.72E-4     0.5     45
SAVE SURFACE 4
SURFACE 5 # Clay/Quartz mixture 4 quartz: 1 illite
    Si_OH   1E-4     0.5    24
    Al_OH   4E-4    20  6
SAVE SURFACE 5
SURFACE 6 #Quartz Surface
    Si_OH   1.72E-4     0.5     45
SAVE SURFACE 6
SURFACE 7 # Quartz + Goethite
    Si_OH   1.53E-03     0.5    28
    Fe_OH 1E-3   200    0.155
SAVE SURFACE 7
SURFACE 8 #Quartz Surface
    Si_OH   1.72E-4     0.5     45
SAVE SURFACE 8
SURFACE 9 # Soil surface
    Si_OH   1E-3    0.5     45
    Al_OH   1E-4        20  6
    Fe_OH 1E-3   200    0.155
SAVE SURFACE 9
SURFACE 10 #Quartz Surface
    Si_OH   1.72E-4     0.5     45
SAVE SURFACE 10
EQUILIBRIUM_PHASES 1    #PLAY SAND, CELL 1A
    Quartz
    K-Feldspar
    Autunite-W 0 0
    Schoepite .1 0  # U too low.
SAVE EQUILIBRIUM_PHASES 1
EQUILIBRIUM_PHASES 2    #PLAY SAND, CELL 1B
    Quartz
    K-Feldspar
    Autunite-W 0 0
    Schoepite .1 0
SAVE EQUILIBRIUM_PHASES 2
EQUILIBRIUM_PHASES 3    #SOIL, CELL 2
    Quartz
    Autunite-W 0 0
    Schoepite .1 0
SAVE EQUILIBRIUM_PHASES 3
EQUILIBRIUM_PHASES 4    #PLAY SAND, CELL 3
    Quartz
    K-Feldspar
    Autunite-W 0 0
    Schoepite .1 0
SAVE EQUILIBRIUM_PHASES 4
EQUILIBRIUM_PHASES 5    #QUARTZ + ILLITE, CELL 4
    Quartz
    Illite 2.8 1
    Autunite-W 0 0
```

```
        Schoepite 0 0
    SAVE EQUILIBRIUM_PHASES 5
    EQUILIBRIUM_PHASES 6    #PLAY SAND, CELL 5
        Quartz
        K-Feldspar
        Autunite-W 0 0
        Schoepite .1 0
    SAVE EQUILIBRIUM_PHASES 6
    EQUILIBRIUM_PHASES 7    #QUARTZ + GOETHITE, CELL 6
        Quartz
        Goethite
        Autunite-W 0 0
        Schoepite 0 0
    SAVE EQUILIBRIUM_PHASES 7
    EQUILIBRIUM_PHASES 8    #PLAY SAND, CELL 7
        Quartz
        K-Feldspar
        Autunite-W 0 0
        Schoepite .1 0
    SAVE EQUILIBRIUM_PHASES 8
    EQUILIBRIUM_PHASES 9    #SOIL, CELL 8
        Quartz
        Autunite-W 0 0
        Schoepite .1 0
    SAVE EQUILIBRIUM_PHASES 9
    EQUILIBRIUM_PHASES 10   #PLAY SAND, CELL 9
        Quartz
        K-Feldspar
        Autunite-W 0 0
        Schoepite .1 0
    SAVE EQUILIBRIUM_PHASES 10
    USER_PUNCH
        heading U(ppm)
        10  REM convert to ppm
        20  PUNCH TOT("U")*238*1000
        end
    END
-----------------------------------
    SELECTED_OUTPUT
        reset true
        file a_ornl_phos9.sel
        user_punch true
        ph true
        pe false
        reaction false
        temperature false
        alkalinity false
        ionic_strength false
        water false
        charge_balance false
        percent_error false
        totals U K Fe C #Si Na
        molalities
            UO2+2
            Si_OUO2+
            Si_OUO2(OH)3-2
            Si_O(UO2)3(OH)5
```

```
            Al_OUO2+
            Al_O(UO2)3(OH)5
            (Fe_O)2UO2
            Fe_PO4UO2
        si
            Quartz
            K-feldspar
            Illite
            UO2(OH)2(beta)      #llnl
            CaUO4           #llnl
            UO3:.9H2O(alpha)    #llnl
            B-UO2(OH)2
            Becquerelite
            Clarkeite
            Compreignacite
            Schoepite
            Soddyite
            Uraninite(c)
            Uranophane
            CO2(g)
            Autunite-W
            K-Autunite
            Na-Autunite
            Saleeite
        equilibrium_phases
            B-UO2(OH)2
            Becquerelite
            Clarkeite
            Compreignacite
            Schoepite
            Soddyite
            Uraninite(c)
            Uranophane
            Autunite
            Autunite-W
            K-Autunite
            Na-Autunite
            Saleeite
    END
------------------
    SOLUTION 1-10 background ORNL GW
        pH      7.2
        units mmol/L
        Mg  1.10
        S(6)    0.66
            Ca  3.34
        N(+5)   6.68 charge
        K   0.14
            Na      1.29
            Cl      2.31
    EQUILIBRIUM_PHASES
        O2(g)   -0.7
        CO2(g)  -6.5
    END
------------------
SOLUTION 0 background ORNL GW + U + PO41
    pH      7.4
```

```
    -units mmol/L
    Mg      1.10
    S(6)    0.66
        Ca  3.34
    N(+5)   6.68 charge
    K   0.14
        Na      1.295
        Cl      2.31
        U(6)    0.1
        P   0.005
EQUILIBRIUM_PHASES 10
    O2(g)   -0.7
    CO2(g)  -6.5
SAVE SOLUTION 0
PRINT
      -selected_output false
END
------------------
TRANSPORT
        -cells                10
        -shifts               10
        -lengths              .01 .01 .02
        -time_step            8640
        -flow_direction       forward
        -boundary_condition   flux flux
        -dispersivity         0.08
        -correct_disp         true
        -diffusion_coef       0.3e-9
        -print_cells          1-10
        -print_frequency      1
        -punch_cells          1-10
        -punch_frequency      5
PRINT
      -selected_output true
END
------------------
TRANSPORT
        -shifts               60          # unitless time steps, PV = shift/cells
PRINT
      -selected_output true
END
------------------
SOLUTION 0 background ORNL GW + U + PO42
    pH      7.4
    -units mmol/L
    Mg  1.10
    S(6)    0.66
    Ca  3.34
    N(+5)   6.68 charge
    K   0.14
    Na      1.30
    Cl      2.31
    U(6)    0.1
    P   0.01
EQUILIBRIUM_PHASES 10
    O2(g)   -0.7
    CO2(g)  -6.5
```

```
SAVE SOLUTION 0
PRINT
      -selected_output false
END
------------------
TRANSPORT
        -shifts               80          # unitless time steps, PV = shift/cells
PRINT
      -selected_output true
END
------------------
SOLUTION 0 background ORNL GW + U + PO43
    pH      7.4
    -units mmol/L
    Mg  1.10
    S(6)    0.66
    Ca  3.34
    N(+5)   6.68 charge
    K   1.14
        Na      1.35
        Cl      2.31
        U(6)    0.1
        P   0.05
EQUILIBRIUM_PHASES 10
    O2(g)   -0.7
    CO2(g)  -6.5
SAVE SOLUTION 0
PRINT
      -selected_output false
END
------------------
TRANSPORT
        -shifts               60          # unitless time steps, PV = shift/cells
PRINT
      -selected_output true
END
------------------
```

DOE/SC0001389 Final technical report: Investigation of uranium attenuation and release at column and pore scales in response to advective geochemical gradients

pH column model

```
   Input file: a_ornl_ph3
  Output file: a_ornl_ph3.out
Database file: database/wateq4f_testU.dat

------------------
    SOLUTION_MASTER_SPECIES
    SOLUTION_SPECIES
    PHASES
    EXCHANGE_MASTER_SPECIES
    EXCHANGE_SPECIES
    SURFACE_MASTER_SPECIES
    SURFACE_SPECIES
    RATES
    END
------------------

    TITLE Sorption of uranium
    SURFACE_MASTER_SPECIES
        Si_ Si_OH   #Quartz
        Soilx_w Soilx_wOH #Soil weak site (KSS adaptation)
        Soilx_s Soilx_sOH #Soil strong site (KSS adaptation)
        Al_ Al_OH #clay
        Hfo_w Hfo_wOH
        Hfo_s  Hfo_sOH
    SURFACE_SPECIES
        Si_OH = Si_OH
        log_k 0.0
        Si_OH = Si_O- + H+
        log_k -7.6              #Korichi 2009 log K = -7.06
        Si_OH + H+ = Si_OH2+
        log_k -1.24
        Si_OH + UO2+2 = Si_OUO2+ + H+
        log_k -0.30             #Korici 2009 log K = 0.146
        Si_OH + UO2+2 + 3H2O = Si_OUO2(OH)3-2 + 4H+
        log_k -18.7
        Soilx_wOH = Soilx_wOH
        log_k 0.0
        Soilx_wOH + UO2+2  =  Soilx_wOUO2+ + H+
        log_K      3.52
        Soilx_wOH + UO2+2 + 2CO3-2  =  Soilx_wOUO2(CO3)2-3  +  H+
        log_K      13.336
        Soilx_sOH = Soilx_sOH
        log_k 0.0
        Soilx_sOH + UO2+2  =  Soilx_sOUO2+ + H+
        log_K      7.91
        Soilx_sOH + UO2+2 + 2CO3-2  =  Soilx_sOUO2(CO3)2-3  +  H+
        log_K      18.176
        Al_OH=Al_OH
        log_k 0.0
        Si_OH + 3UO2+2 + 5H2O = Si_O(UO2)3(OH)5 + 6H+
        log_k -16.8
        Al_OH + H+ = Al_OH2+
```

```
    log_k 7.6
    Al_OH = Al_O-+ H+
    log_k -10.6
    Al_OH + UO2+2 = Al_OUO2+ + H+
    log_k 2.47
    Al_OH + 3UO2+2 + 5H2O = Al_O(UO2)3(OH)5 + 6H+
    log_k -17.7
    Hfo_wOH=Hfo_wOH
    log_k 0.0
    Hfo_sOH=Hfo_sOH
    log_k 0.0
    Hfo_wOH + H+ =Hfo_wOH2+
    log_k 7.29
    Hfo_sOH + H+ = Hfo_sOH2+
    log_k 7.29
    Hfo_wOH = Hfo_wO-+ H+
    log_k -8.93
    Hfo_sOH = Hfo_sO-+ H+
    log_k -8.93
    Hfo_wOH + CO3-2 + H+ = Hfo_wOCO2-+ H2O
    log_k 12.78
    Hfo_sOH + CO3-2+ H+ = Hfo_sOCO2-+ H2O
    log_k 12.78
    Hfo_wOH + CO3-2+ 2H+ = Hfo_wOCO2H + H2O
    log_k 20.37
    Hfo_sOH + CO3-2+ 2H+ =Hfo_sOCO2H + H2O
    log_k 20.37
    2Hfo_wOH + UO2+2 = (Hfo_wO)2UO2 + 2H+
    log_k -6.06
    2Hfo_sOH + UO2+2 =(Hfo_sO)2UO2 + 2H+
    log_k -2.35
    2Hfo_wOH + UO2+2+ CO3-2 =(Hfo_wO)2UO2CO3-2+ 2H+
    log_k -0.24
    2Hfo_sOH + UO2+2+ CO3-2 =(Hfo_sO)2UO2CO3-2+ 2H+
    log_k 4.33
SURFACE 1 #Quartz Surface
    Si_OH   2E-4    0.5     25
SAVE SURFACE 1
SURFACE 2 #Quartz Surface
    Si_OH   2E-4    0.5     25
SAVE SURFACE 2
SURFACE 3 # Soil surface, need to assess Tx & Sx parameters
    Si_OH   1E-3    0.5     45
    Al_OH   1E-3        20  6
    Hfo_wOH 1E-03   200     0.155
    Hfo_sOH 1E-04                   #assumes 10 weak sites per strong site
SAVE SURFACE 3
SURFACE 4 #Quartz Surface
    Si_OH   1.72E-4     0.5     45
SAVE SURFACE 4
SURFACE 5 # Clay/Quartz mixture 4 quartz: 1 illite
    Si_OH   1E-4     0.5    24
    Al_OH   4E-4    20  6
SAVE SURFACE 5
SURFACE 6 #Quartz Surface
    Si_OH   1.72E-4     0.5     45
SAVE SURFACE 6
```

```
SURFACE 7 # Quartz + Goethite
    Si_OH   1.53E-03     0.5    28
    Hfo_wOH 3.1E-04     200     0.155
    Hfo_sOH 3.1E-06                 #assumes 100 weak sites per strong site
SAVE SURFACE 7
SURFACE 8 #Quartz Surface
    Si_OH   1.72E-4     0.5     45
SAVE SURFACE 8
SURFACE 9 # Soil surface
    Si_OH   1E-3    0.5     45
    Al_OH   1E-4        20  6
    Hfo_wOH 1E-03   200     0.155
    Hfo_sOH 1E-05                   #assumes 100 weak sites per strong site
SAVE SURFACE 9
SURFACE 10 #Quartz Surface
    Si_OH   1.72E-4     0.5     45
SAVE SURFACE 10
EQUILIBRIUM_PHASES 1    #PLAY SAND, CELL 1A
    Quartz
    K-Feldspar
    B-UO2(OH)2  0 0     # THIS LOOKS PRETTY GOOD.
    Schoepite 0 0   # U too low.
SAVE EQUILIBRIUM_PHASES 1
EQUILIBRIUM_PHASES 2    #PLAY SAND, CELL 1B
    Quartz
    K-Feldspar
    B-UO2(OH)2  0 0
    Schoepite 0 0
SAVE EQUILIBRIUM_PHASES 2
EQUILIBRIUM_PHASES 3    #SOIL, CELL 2
    Quartz
    B-UO2(OH)2  0 0
    Schoepite 0 0
SAVE EQUILIBRIUM_PHASES 3
EQUILIBRIUM_PHASES 4    #PLAY SAND, CELL 3
    Quartz
    K-Feldspar
    B-UO2(OH)2  0 0
    Schoepite 0 0
SAVE EQUILIBRIUM_PHASES 4
EQUILIBRIUM_PHASES 5    #QUARTZ + ILLITE, CELL 4
    Quartz
    Illite -.1 1
    B-UO2(OH)2  0 0
    Schoepite 0 0
SAVE EQUILIBRIUM_PHASES 5
EQUILIBRIUM_PHASES 6    #PLAY SAND, CELL 5
    Quartz
    K-Feldspar
    B-UO2(OH)2  0 0
    Schoepite 0 0
SAVE EQUILIBRIUM_PHASES 6
EQUILIBRIUM_PHASES 7    #QUARTZ + GOETHITE, CELL 6
    Quartz
    Goethite
    B-UO2(OH)2  0 0
    Schoepite .1 0
```

```
        Schoepite 0 0
    SAVE EQUILIBRIUM_PHASES 7
    EQUILIBRIUM_PHASES 8    #PLAY SAND, CELL 7
        Quartz
        K-Feldspar
        B-UO2(OH)2  0 0
        Schoepite 0 0
    SAVE EQUILIBRIUM_PHASES 8
    EQUILIBRIUM_PHASES 9    #SOIL, CELL 8
        Quartz
        B-UO2(OH)2  0 0
        Schoepite 0 0
    SAVE EQUILIBRIUM_PHASES 9
    EQUILIBRIUM_PHASES 10   #PLAY SAND, CELL 9
        Quartz
        K-Feldspar
        B-UO2(OH)2  0 0
        Schoepite 0 0
    SAVE EQUILIBRIUM_PHASES 10
    USER_PUNCH
        heading U(ppm)
        10  REM convert to ppm
        20  PUNCH TOT("U")*238*1000
        end
    END
------------------
    SELECTED_OUTPUT
        reset true
        file a_ornl_pH3.sel
        user_punch true
        ph true
        pe false
        reaction false
        temperature false
        alkalinity false
        ionic_strength false
        water false
        charge_balance false
        percent_error false
        totals U K Fe C #Si Na
        molalities
            UO2+2
            Si_OUO2+
            Si_OUO2(OH)3-2
            Si_O(UO2)3(OH)5
            Soilx_wOUO2+
            Soilx_sOUO2+
            Soilx_wOUO2(CO3)2-3
            Soilx_sOUO2(CO3)2-3
            Al_OUO2+
            Al_O(UO2)3(OH)5
            (Hfo_wO)2UO2
            (Hfo_sO)2UO2
            (Hfo_wO)2UO2CO3-2
            (Hfo_sO)2UO2CO3-2
        si
            Quartz
```

```
            K-feldspar
            Illite
            UO2(OH)2(beta)      #llnl
            CaUO4               #llnl
            UO3:.9H2O(alpha)    #llnl
            B-UO2(OH)2
            Becquerelite
            Clarkeite
            Compreignacite
            Schoepite
            Soddyite
            Uraninite(c)
            Uranophane
            CO2(g)
        equilibrium_phases
            B-UO2(OH)2
            Becquerelite
            Clarkeite
            Compreignacite
            Schoepite
            Soddyite
            Uraninite(c)
            Uranophane
    END
------------------
    SOLUTION 1-10 background ORNL GW
        pH      7.2
        units mmol/L
        Mg      1.10
        S(6)    0.66
        Ca      3.34
        N(+5)   6.68 charge
        K       0.14
        Na      1.29
        Cl      2.31
    EQUILIBRIUM_PHASES 100
        O2(g)   -0.7
        CO2(g)  -6.5
    END
------------------
SOLUTION 0 background ORNL GW + U + pH4
    pH      4
    -units mmol/L
    Mg      1.10
    S(6)    0.66
    Ca      3.34
    N(+5)   6.68 charge
    K       0.16
    Na      1.29
    Cl      2.31
    U(6)    0.1
EQUILIBRIUM_PHASES 10
    O2(g)   -0.7
    CO2(g)  -6.5
SAVE SOLUTION 0
PRINT
      -selected_output false
```

```
END
------------------
TRANSPORT
        -cells                10
        -shifts               10
        -lengths              .01 .01 .02
        -time_step            8640
        -flow_direction       forward
        -boundary_condition   flux flux
        -dispersivity         0.08
        -correct_disp         true
        -diffusion_coef       0.3e-9
        -print_cells          1-10
        -print_frequency      1
        -punch_cells          1-10
        -punch_frequency      5
PRINT
      -selected_output true
END
------------------
TRANSPORT
        -shifts               60          # unitless time steps, PV = shift/cells
PRINT
      -selected_output true
END
------------------
SOLUTION 0 background ORNL GW + U + pH6
    pH      6
    -units mmol/L
    Mg      1.10
    S(6)    0.66
    Ca      3.34
    N(+5)   6.68 charge
    K       0.24
    Na      1.29
    Cl      2.31
    U(6)    0.1
EQUILIBRIUM_PHASES 10
    O2(g)   -0.7
    CO2(g)  -6.5
SAVE SOLUTION 0
PRINT
      -selected_output false
END
------------------
TRANSPORT
        -shifts               80          # unitless time steps, PV = shift/cells
PRINT
      -selected_output true
END
------------------
SOLUTION 0 background ORNL GW + U + pH8
    pH      8
    -units mmol/L
    Mg      1.10
    S(6)    0.66
    Ca      3.34
```

```
    N(+5)   6.68 charge
    K       1.14
    Na      1.29
    Cl      2.31
    U(6)    0.1
EQUILIBRIUM_PHASES 10
    O2(g)   -0.7
    CO2(g)  -6.5
SAVE SOLUTION 0
PRINT
      -selected_output false
END
-----------------
TRANSPORT
        -shifts               60          # unitless time steps, PV = shift/cells
PRINT
      -selected_output true
END
-----------------
```